

Journal of Visualized Experiments

Real-time fluorescent measurement of synaptic functions in models of amyotrophic lateral sclerosis --Manuscript Draft--

Article Type:	Invited Methods Collection - JoVE Produced Video
Manuscript Number:	JoVE62813R1
Full Title:	Real-time fluorescent measurement of synaptic functions in models of amyotrophic lateral sclerosis
Corresponding Author:	Brigid Jensen UNITED STATES
Corresponding Author's Institution:	
Corresponding Author E-Mail:	Brigid.Jensen@jefferson.edu
Order of Authors:	Karthik Krishnamurthy Davide Trotti Piera Pasinelli Brigid Jensen
Additional Information:	
Question	Response
Please specify the section of the submitted manuscript.	Neuroscience
Please indicate whether this article will be Standard Access or Open Access.	Standard Access (\$1400)
Please indicate the city, state/province, and country where this article will be filmed . Please do not use abbreviations.	Philadelphia, PA, USA
Please confirm that you have read and agree to the terms and conditions of the author license agreement that applies below:	I agree to the Author License Agreement
Please provide any comments to the journal here.	

TITLE:

Real-Time Fluorescent Measurement of Synaptic Functions in Models of Amyotrophic Lateral Sclerosis

AUTHORS AND AFFILIATIONS:

Karthik Krishnamurthy^{*#}, Davide Trotti, Piera Pasinelli, Brigid Jensen^{*#}

Jefferson Weinberg ALS Center, Thomas Jefferson University, Philadelphia PA, USA

*These authors contributed equally to this work.

Email addresses of the authors:

Karthik Krishnamurthy (Karthik.Krishnamurthy@jefferson.edu)

Davide Trotti (Davide.Trotti@jefferson.edu)

Piera Pasinelli (Piera.Pasinelli@jefferson.edu)

Brigid Jensen (Brigid.Jensen@jefferson.edu)

Email addresses of corresponding authors:

Karthik Krishnamurthy (Karthik.Krishnamurthy@jefferson.edu)

Brigid Jensen (Brigid.Jensen@jefferson.edu)

SUMMARY:

Two related methods are described to visualize subcellular events required for synaptic transmission. These protocols enable the real-time monitoring of the dynamics of presynaptic calcium influx and synaptic vesicle membrane fusion using live-cell imaging of *in vitro* cultured neurons.

ABSTRACT:

Before neuronal degeneration, the cause of motor and cognitive deficits in patients with amyotrophic lateral sclerosis (ALS) and/or frontotemporal lobe dementia (FTLD) is dysfunction of communication between neurons and motor neurons and muscle. The underlying process of synaptic transmission involves membrane depolarization-dependent synaptic vesicle fusion and the release of neurotransmitters into the synapse. This process occurs through localized calcium influx into the presynaptic terminals where synaptic vesicles reside. Here, the protocol describes fluorescence-based live-imaging methodologies that reliably report depolarization-mediated synaptic vesicle exocytosis and presynaptic terminal calcium influx dynamics in cultured neurons.

Using a styryl dye that is incorporated into synaptic vesicle membranes, the synaptic vesicle release is elucidated. On the other hand, to study calcium entry, Gcamp6m is used, a genetically encoded fluorescent reporter. We employ high potassium chloride-mediated depolarization to mimic neuronal activity. To quantify synaptic vesicle exocytosis unambiguously, we measure the loss of normalized styryl dye fluorescence as a function of time. Under similar stimulation conditions, in the case of calcium influx, Gcamp6m fluorescence increases. Normalization and quantification of this fluorescence change are performed in a similar manner to the styryl dye

protocol. These methods can be multiplexed with transfection-based overexpression of fluorescently tagged mutant proteins. These protocols have been extensively used to study synaptic dysfunction in models of *FUS*-ALS and *C9ORF72*-ALS, utilizing primary rodent cortical and motor neurons. These protocols easily allow for rapid screening of compounds that may improve neuronal communication. As such, these methods are valuable not only for the study of ALS but for all areas of neurodegenerative and developmental neuroscience research.

INTRODUCTION:

Modeling amyotrophic lateral sclerosis (ALS) in the laboratory is made uniquely challenging due to the overwhelmingly sporadic nature of over 80% of cases¹, coupled with the vast number of genetic mutations known to be disease-causative². Despite this, all cases of ALS share the unifying feature that before outright neuronal degeneration, there is dysfunctional communication between presynaptic motor neurons and postsynaptic muscle cells^{3,4}. Clinically, as patients lose connectivity of the remaining upper and lower motor neurons, they present with features of neuronal hyper- and hypoexcitability throughout the disease⁵⁻⁹, reflecting complex underlying molecular changes to these synapses, which we, as ALS researchers, seek to understand.

Multiple transgenic models have illustrated that deterioration and disorganization of the neuromuscular junction occur with the expression of ALS-causative genetic mutations, including *SOD1*¹⁰, *FUS*^{11,12}, *C9orf72*¹³⁻¹⁶, and *TDP43*¹⁷⁻¹⁹ through morphological assessments, including evaluation of synaptic boutons, spine densities, and pre/postsynaptic organization. Mechanistically, since the landmark papers of Cole, Hodgkin, and Huxley in the 1930s, it has also been possible to evaluate synaptic responses through electrophysiological techniques in either *in vitro* cell culture or tissue slice preparations²⁰. Through these strategies, many models of ALS have demonstrated synaptic transmission deficits. For example, a mutant variant of *TDP43* causes enhanced firing frequency and decreases action potential threshold in NSC-34 (spinal cord x neuroblastoma hybrid cell line 34) motor-neuron-like cells²¹. This same variant also causes dysfunctional synaptic transmission at the neuromuscular junction (NMJ) before the onset of behavioral motor deficits in a mouse model²². It was previously showed that mutant *FUS* expression results in reduced synaptic transmission at the NMJ in a drosophila model of *FUS*-ALS before locomotor defects¹¹. A recent report using induced pluripotent stem cells derived from *C9orf72*-expansion carriers revealed a reduction in the readily releasable pool of synaptic vesicles²³. Altogether, these studies and others highlight the importance of building a more comprehensive understanding of the mechanisms underlying synaptic signaling in disease-relevant models of ALS. This will be pivotal in understanding the pathobiology of ALS and developing potential therapeutic targets for patients.

Methods of current and voltage clamping cells have been invaluable in determining membrane properties such as conductance, resting membrane potential, and quantal content of individual synapses^{20,24}. However, one of the significant limitations of electrophysiology is that it is technically challenging and only provides insights from a single neuron at a time. Live-cell confocal microscopy, coupled with specific fluorescent probes, offers the opportunity to investigate the synaptic transmission of neurons in a spatiotemporal manner²⁵⁻²⁷. Although not a direct measure of neuronal excitability, this fluorescence approach can provide a relative

measurement of two molecular correlations of synaptic function: synaptic vesicle release and calcium transients at synaptic terminals.

When an action potential reaches the presynaptic terminal region of neurons, calcium transients are triggered, facilitating the transition from an electrical signal to the process of neurotransmitter release²⁸. Voltage-gated calcium channels localized to these areas tightly regulate calcium signaling to modulate the kinetics of neurotransmitter release²⁹. The first reported fluorescence-based recordings of calcium transients were performed using either the dual-wavelength indicator Fura-2 AM or the single wavelength dye Fluo-3 AM^{30–32}. While these dyes offered great new insight at the time, they suffer from several limitations such as non-specific compartmentalization within cells, active or passive dye loss from labeled cells, photobleaching, and toxicity if imaged over extended periods of time³³. In the past decade, genetically encoded calcium indicators have become the workhorses for imaging various forms of neuronal activity. These indicators combine a modified fluorescent protein with a calcium chelator protein that rapidly switches fluorescence intensity after the binding of Ca^{2+} ions³⁴. The application of these new indicators is vast, allowing for much easier visualization of intracellular calcium transients both in *in vitro* and *in vivo* settings. One family of these genetically encoded reporters, known as GCaMP, are now broadly utilized. These indicators contain a C-terminal calmodulin domain, followed by green fluorescent protein (GFP), and are capped by an N-terminal calmodulin-binding region^{35,36}. Calcium-binding to the calmodulin domain triggers an interaction with the calmodulin-binding region, resulting in a conformational change in the overall protein structure and a substantial increase in the fluorescence of the GFP moiety^{35,36}. Over the years, this family of reporters has undergone several evolutions to enable distinct readouts for particular calcium transients with specific kinetics (slow, medium, and fast), each with slightly different properties^{37,38}. Here, the usage of the reporter GcaMP6 has been highlighted, which has been previously shown to detect single action potentials and dendritic calcium transients in neurons both *in vivo* and *in vitro*³⁷.

Calcium transients in the presynaptic region trigger synaptic vesicle fusion events, causing neurotransmitter release into the synapse and initiation of signaling events in the postsynaptic cell^{28,39}. Synaptic vesicles are both rapidly released and recycled, as the cell homeostatically maintains a stable cell membrane surface area and readily releasable pool of fusion capable membrane-bound vesicles⁴⁰. The styryl dye used here has an affinity toward lipid membranes and specifically changes its emission properties based on the ordering of the surrounding lipid environment^{41,42}. Thus, it is an ideal tool for labeling recycling synaptic vesicles and subsequent tracking of these vesicles as they are later released following neuronal stimulation^{41,42}. The protocol that has been generated and optimized is an adaptation of the concepts described initially by Gaffield and colleagues, which allows us to visualize styryl dye-labeled synaptic vesicle puncta over time continuously⁴¹.

Here, two related fluorescence-based methodologies are described, reliably reporting specific cellular events involved in synaptic transmission. Protocols have been defined to probe the dynamics of depolarization-mediated presynaptic terminal calcium influx and synaptic vesicle exocytosis in cultured neurons. Here, methods and representative results are focused on using

primary rodent cortical or motor neurons as the *in vitro* model system, as there are published studies using these cell types^{43,44}. However, these methods are also applicable to differentiated human i³ cortical-like neurons⁴⁵, as we have also had success with both protocols in presently ongoing experimentation in our laboratory. The general protocol is outlined in a stepwise linear format, shown in **Figure 1**. In brief, to study calcium dynamics in neurites, mature neurons are transfected with plasmid DNA to express the fluorescent reporter GCaMP6m under a Cytomegalovirus (CMV) promoter^{37,46}. Transfected cells have a low level of basal green fluorescence, which increases in the presence of calcium. Regions of interest are specified to monitor fluorescence changes throughout our manipulation. This allows for highly spatially and temporally localized fluctuations in calcium to be measured^{37,46}. For evaluating synaptic vesicle fusion and release, mature neurons are loaded with styryl dye incorporated into synaptic vesicle membranes as they are recycled, reformed, and reloaded with neurotransmitters in presynaptic cells^{41–43,47,48}. The current dyes used for this purpose label synaptic vesicles along neurites and are used as a proxy for these regions in live-imaging experiments, as was shown by co-staining of styryl dye and synaptotagmin by Kraszewski and colleagues⁴⁹. Included here are representative images of similar staining that have also been performed (**Figure 2A**). Previous investigators have extensively used such dyes to report synaptic vesicle dynamics at the neuromuscular junction and hippocampal neurons^{48–56}. By selecting punctate regions of dye-loaded vesicles and by monitoring decreases in fluorescence intensity following vesicle release, functional synaptic transmission capacity and temporal dynamics of release can be studied following stimulation⁴³. For both methods, a medium containing a high concentration of potassium chloride is employed to depolarize cells to mimic neuronal activity. Imaging parameters are specified to capture sub-second intervals spanning a baseline normalization followed by our stimulation capture period. Fluorescence measurements at each time point are determined, normalized to the background, and quantified over the experimental time period. Calcium-influx mediated GCaMP6m fluorescence increase or effective synaptic vesicle exocytosis styryl dye release fluorescence decrease can be detected through this strategy. Detailed methodological setup and parameters for these two protocols and a discussion on their advantages and limitations are described below.

[Place Figure 1 here]

PROTOCOL:

All animal procedures performed in this study were approved by the Institutional Animal Care and Use Committee of Jefferson University.

1. Primary culture of neurons from embryonic rat cortex

NOTE: Primary cortical neurons are isolated from E17.5 rat embryos as previously described^{57,58}. No strain bias appears to exist with the success of this culturing protocol. This method is described briefly below. The previous articles indicated should be referenced for complete details.

1.1 Euthanize pregnant female rats by CO₂ inhalation followed by secondary confirmation by cervical dislocation.

177
178 1.2 Harvest embryos and isolate brains in ice-cold 20 mM HEPES-buffered Hank's balanced
179 salt solution (HBSS). From the outer cortex shell, separate and then discard striatum and
180 hippocampi. Collect cortices.

181
182 1.3 Use fine forceps to remove meninges from cortices. To do this, hold the cortex in place
183 with one pair of closed forceps using gentle pressure.

184
185 NOTE: With the second pair of forceps in the second hand, pinch meninges. Peel away meninges
186 using rolling motion with pinched pair. Reposition with the closed forceps and repeat as
187 necessary until meninges is entirely removed.

188
189 1.4 Incubate cortices with 10 µg/mL of papain in HBSS for 4 min at 37 °C.

190
191 1.5 Wash three times in HBSS, and then triturate gently 5-10 times with a fire-polished glass
192 Pasteur pipette to obtain a homogenous cell suspension.

193
194 NOTE: Avoid bubbles; maintain the pipette within the cell suspension.

195
196 1.6 Plate neurons on 100 µg/mL poly-D-lysine coated 35 mm glass-bottom dishes at a density
197 of 75,000 cells/dish in neurobasal medium with B27 supplement (2%), and penicillin-
198 streptomycin.

200 **2. Primary culture of motor neurons from embryonic rat spinal cord**

201
202 NOTE: Primary motor neurons are prepared from E13.5 rat embryos as previously described, with
203 few modifications^{59,60}. No strain bias appears to exist with the success of this culturing protocol.
204 This method is described briefly below. The preceding articles indicated should be referenced for
205 complete details.

206
207 2.1 Euthanize pregnant female rats as in step 1.1.

208
209 2.2 Dissect 10–20 spinal cords from embryos and break into small fragments mechanically
210 using two pairs of forceps to pinch and pull, respectively.

211
212 2.3 Incubate in 0.025% trypsin for 8 min, followed by addition of DNase at 1 mg/mL.

213
214 2.4 Centrifuge through a 4% w/v BSA cushion at 470 x *g* for 5 min at 4 °C with no break.

215
216 2.5 Centrifuge pelleted cells for 55 min at 830 x *g* at 4 °C without brake through a 10.4% (v/v)
217 density gradient medium (see **Table of Materials**) cushion. Carry forward the motor neuron band
218 at the visual interface.

NOTE: To ensure capture of all cells, use phenol-free media for the density gradient step and phenol-containing media for all the other steps. The interface of the density gradient and dissociation media is easily identifiable based on the color difference.

2.6 Spin collected bands through another 4% w/v BSA cushion at 470 x *g* for 5 min at 4 °C with no break.

2.7 Resuspend purified motor neurons in complete neurobasal medium with B27 supplement (2%), glutamine (0.25%), 2-mercaptoethanol (0.1%), horse serum (2%), and penicillin-streptomycin.

2.8 Plate neurons on 100 µg/mL of poly-lysine and 3 µg/mL of laminin-coated coverslips at a density of 50,000 cells/35 mm glass-bottom dish.

3. Neuronal transfections

NOTE: This step is carried out for neurons that will undergo GCaMP calcium imaging and/or neurons. An exogenous protein or RNA of interest is introduced in advance of synaptic evaluation. In contrast, styryl dye is loaded just before the imaging session and is addressed in section 6. The summary below is the transfection protocol used for primary rodent neurons in the presented examples, but it can easily be adapted and optimized to the user's needs.

3.1 Transfections for cultured primary cortical neurons occur at day 12 *in vitro* (DIV 12), whereas motor neurons are transfected at day 7 *in vitro* (DIV 7).

NOTE: All the following steps occur within an aseptic biosafety cabinet.

3.2 Transfect 500 ng of GCaMP6m using transfection reagent at a ratio of 1:2 by volume. For co-transfections, add a total of 1.25 µg of total DNA/dish, maintaining this DNA to reagent ratio.

NOTE: In the experimental examples shown, 750 ng of ALS/FTD-related plasmid of interest has been transfected to express C9orf72-ALS linked dipeptides, mutant FUS protein, etc. Ensure that the fluorescent tag of the co-transfected plasmid will not conflict with the FITC channel of GCaMP imaging. Likewise, if doing styryl dye imaging, ensure that the co-transfected plasmid will not conflict with the TRITC channel of imaging. Usage of synaptophysin-GCaMP3 is equally effective in this protocol. Therefore, transfect the same amount of this plasmid and follow all the steps as usual in section 7.

3.3 Incubate the DNA-transfection reagent complex at room temperature for 10 min.

3.4 Gently add the incubated complex to neurons dropwise with swirling. Return the dish to CO₂ incubator at 37 °C for 45–60 min.

3.5 Remove the entire culture media containing the DNA-transfection reagent complex and replace it with a 50–50 by volume preparation of pre-conditioned and fresh neuronal media. Then, put cells back into the CO₂ incubator for 48 h until imaging.

4. Preparation of buffer solutions and styryl dye stock solution

4.1 Make low and high aCSF solutions fresh before imaging using the ingredients listed in **Table 1**. Filter both the buffer solutions before use.

NOTE: CaCl₂ dihydrate can form Ca(OH)₂ upon storage. For maximum efficacy, always use a recently opened container. If this is not possible, to remove Ca(OH)₂ from the external surface and ensure maximum solubility, solutions may be carbonated with gaseous CO₂ for 5 min before CaCl₂ addition. If this step is taken, adjust the pH of the resulting solution to maintain a pH value of 7.4, as excessive carbonation will result in Ca(HCO₃)₂ formation.

[Place Table 1 here]

4.2 Prepare styryl dye stock solution by taking a 100 µg vial of dye and reconstituting it to a stock concentration of 10 mM with distilled water or neurobasal medium.

5. Microscope and perfusion system setup

NOTE: For imaging glass-bottom Petri dishes, an inverted confocal fluorescence microscope is preferred due to the flexibility of perfusion and for the use of a high numerical aperture oil immersion objective. Refer to the **Table of Materials** for the confocal microscope, camera, and objectives used for imaging of examples detailed in the **Representative Results** section.

5.1 Perform all the experiments at 37 °C with constant 5% CO₂ levels using an incubator system-coupled stage mount.

5.2 Control image acquisition using confocal software. Optimize acquisition settings at the start of the imaging session to choose excitation power and gain to ensure optimal visualization of signals without photobleaching.

5.2.1 Keep excitation power, exposure time, detector gain and frame rate constant across all samples. Carry out time-lapse imaging using an aspect ratio of 512 x 512 and frame rate of 2 images/s to minimize dye bleaching.

NOTE: While puncta should be clearly visible, laser intensity should be set to the minimum possible to avoid bleaching and phototoxicity. Set the confocal aperture to the narrowest setting to achieve optimal resolution of fluorescent puncta within neurites. Exposure time is set to 200 ms or less, consistent across samples. The maximum imaging speed of the camera used was 2 images/s. If using a faster camera, more images/s can be taken. Temporal imaging settings should be chosen if possible.

5.3 Select the following fluorescence excitation/dichroic/emission filter combinations for imaging using confocal software: Gcamp6m/Gcamp3 with FITC and styryl dye with TRITC, respectively.

5.4 Use the perfect focus feature of the confocal imaging acquisition software during time-lapse imaging to avoid z-drift.

NOTE: Due to the rapid speed of imaging, a single plane is imaged. Ensuring the lack of z-drift during the experiment is very important.

5.5 Select the **Time** tab in the image acquisition panel to set the recording periods and intervals.

5.5.1 Set **Phase #1** to **Interval 500 ms, Duration 3–5 min.**

5.5.2 Set **Phase #2** to **Interval 500 ms, Duration 5 min.**

NOTE: Phase #1 corresponds to baseline recording, Phase #2 to the stimulation period, respectively.

5.6 Assemble gravity perfusion apparatus for aCSF using a valve control system and a channel manifold.

5.6.1 Load high KCl (see **Table 1**) into a 50 mL syringe at the top of the apparatus, with tubing running through the system. Set the flow rate to 1 mL/min.

5.7 Load a 35 mm glass dish containing neurons onto the confocal imaging stage, with the end of the perfusion tubing placed at the dish edge. Choose the field for imaging.

6. **Styryl dye imaging of synaptic vesicle release**

6.1 Incubate cells in low KCl aCSF (see **Table 1**) for 10 min at 37 °C, 48 h post-transfection.

6.2 Load primary cortical or motor neurons on glass-bottom Petri dishes with styryl dye.

6.2.1 Remove low KCl aCSF by aspiration.

6.2.2 Use a pipette to load neurons in the dark with 10 μ M of styryl dye in aCSF containing 50 mM KCl for 5 min.

6.2.3 Remove the loading solution and bath neurons in low KCl aCSF for 10 min to eliminate non-specific dye loading.

6.3 Place the 35 mm glass-bottom dish onto the imaging stage, and then observe either under a 20x air objective or 40x oil immersion objective of an inverted confocal microscope.

NOTE: Use GFP fluorescence to locate transfected cells in case of cells co-transfected with a GFP-tagged plasmid.

6.4 Excite styryl dye using a 546 nm laser, collect emission using a 630–730 nm (TRITC) bandpass filter.

6.5 Select the imaging field and engage perfect focus. Next, take a single still image with brightfield, TRITC, and fluorescence marker channels to mark neuronal boundaries.

6.6 Initiate **Run Now** in the acquisition software. Carry out the basal recording for 3–5 min to exclude variations in dye intensity, if any (Phase #1).

NOTE: It is essential to ensure that any decrease in dye intensity is due to synaptic vesicle release and not passive dye diffusion or photobleaching. This 3–5 min pre-stimulation period should result in a steady and maintained dye intensity level. The final 30 s of this recording will be used to determine a mean baseline fluorescence value for each ROI. Before evaluating experimental conditions, an additional non-stimulation condition of approximately 10 min of continuous recording using the intended acquisition settings can also be performed to ensure steady fluorescence values using the laser settings for an extended period.

6.7 At the switch to Phase #2, trigger **On** the button for the perfusion system. Then, constantly perfuse 50 mM KCl to neurons to facilitate dye unloading (Phase #2).

6.7.1 Carry out recordings for 300 s after KCl addition. After this, acquisition stops; trigger the **Off** switch for the perfusion system.

6.8 Save the experiment and analyze data using confocal software as described in section 8 below.

NOTE: The experiment may be stopped at this point, and analysis can be performed later. In the case where cells do not require transfection for the expression of proteins of interest, this protocol may be performed at any timepoint *in vitro* when seeking to examine the functionality of synaptic unloading. Following a test of control cells to ensure proper synaptic unloading, the experimenter should be blinded to the genetic or pharmacologic conditions of each dish tested to minimize bias.

7. Fluorescence imaging of Gcamp6m calcium transients

7.1 Transfect primary rodent cortical neurons cultured on 35 mm glass-bottom dishes with 500 ng of Gcamp6m as indicated in section 3.

NOTE: If desired, co-transfect neurons with a plasmid of interest containing a fluorescent tag in the red or far-red range.

7.2 Incubate neurons with low KCl aCSF for 15 min 48 h post-transfection and then mount the dish on the imaging platform.

7.3 Visualize GCaMP6m fluorescence using a FITC filter (488 nm) and a 20x or 40x objective.

7.4 Select the imaging field and engage perfect focus. Next, take a single still image with brightfield, FITC, and fluorescence marker channels to mark neuronal boundaries.

7.5 Initiate **Run Now** in the acquisition software. Carry out the baseline recording for 5 min, and then perfuse with aCSF containing 50 mM KCl in the same manner as described in section 6 for styryl dye experiments.

NOTE: The goal of this imaging is to measure evoked calcium transients. Should a neuron have basal firing activity and calcium fluxes during the pre-stimulation period, it is not used in data analysis. Instead, only cells with stable background fluorescence are used. Post-stimulation periods can also be extended to 60 min for calcium transients, with or without additional continuous high KCl perfusion.

7.6 Save the experiment and analyze data using confocal software as described in section 8 below. The experiment may be stopped at this point, and the analysis can be performed later.

NOTE: If the cells do not require transfection for expression of proteins of interest, this protocol may be performed at any timepoint *in vitro* when seeking to examine calcium transients. Following a test of control cells to ensure measurement of calcium transients, the experimenter should be blinded to the genetic or pharmacologic conditions of each dish tested to minimize bias.

8. Image analysis

8.1 Open time-lapse images with confocal software.

8.2 Align images in time-lapse series by the command series: **Image | Processing | Align Current Document**. Select **Align to the First Frame**.

8.3 Select regions of interest (ROIs) along neurites using the ROI selection tool, a bean-shaped icon on the right of the image frame (**Figure 3B**). Also, mark an ROI representing background fluorescence intensity.

NOTE: ROIs are selected by choosing areas of distinctly separated puncta along neuronal tracks indicated by the brightfield still image. At least five ROIs per neuron are chosen for analysis. The background ROI is chosen in a region of the field of view that does not contain neurites.

8.4 Measure raw fluorescence over time for selected ROIs using the following command series: **Measure | Time Measurement**.

8.4.1 Initiate the **Measure** function at the upper portion of the **Time Measurement** panel. A graphical representation of raw fluorescence over time (**Figure 3C**) and quantitative data are both generated.

NOTE: Each data point represents the raw fluorescence for that ROI for the frame associated with that specific measured time point.

8.5 Export raw fluorescence intensities to the spreadsheet software.

8.6 Analyze each ROI independently. First, normalize data by subtracting the background ROI intensity from the ROI of interest intensity at each time point.

8.6.1 Take the raw fluorescence value from the background ROI at each specific time point and subtract this from the ROI of interest raw intensity value at that time point.

NOTE: This is done for the entire recording period, both basal and stimulation phases.

8.7 Determine the average ROI of interest intensity for the last 30 s of baseline.

8.7.1 Average the normalized raw basal values generated in step 8.6 from the final 30 s of the 3–5 min basal recording period.

NOTE: The entire period of basal recording could be used to generate this value. However, as this value stabilizes and is maintained, the 60-time points of the final 30 s are of sufficient sampling size to represent the whole.

8.8 Compare this baseline value to the normalized intensity value at each time point, generating a change in fluorescence (ΔF) value.

8.8.1 Take the value from step 8.7 and subtract the average baseline fluorescent value. Do this and subsequent steps for the entire recording period, both basal and stimulation phases.

8.9 Calculate this change concerning the baseline fluorescence value, generating a change in fluorescence/baseline fluorescence ($\Delta F/F$). To do this, take the value from step 8.8 and divide it by the average baseline fluorescent value.

8.10 Finally, set the starting point value to 1 so that increases or decreases can be easily visualized graphically over time.

8.10.1 Take the value generated in step 8.9 and add 1.

NOTE: When this is done correctly, the 30 s of baseline period values should hover near the value of 1. In cells effectively releasing synaptic content, this value should trend from 1 to 0 following the start of stimulation. An example of steps 6–9 is presented in **Figure 3E**.

9. Data analysis

NOTE: The experimenter can be unblinded to experimental conditions to pool data for analysis appropriately. Use a sample size of at least 10 neurons per condition from each of three independent experiments. Only consider neurons for inclusion if at least five ROI regions can be designated. This level of experimental replication was sufficient in published studies to demonstrate a profound loss of synaptic unloading in ALS-related poly-GA-containing cells versus GFP controls (see **Representative Results**). However, if a more subtle phenotype is observed, the number of biological and/or technical replicates may require optimization by the user.

9.1 Using all calculated $\Delta F/F$ values over time from ROIs of a given experimental condition, determine a mean $\Delta F/F$ value for each time point along with an SEM.

9.2 Plot data using a graphing and statistics software program in xy-format, where x is the time elapsed, and y is the $\Delta F/F$ value calculated in step 9.1. Present all the values as mean \pm SEM.

9.3 To determine statistical significance, use the Student's *t*-test for comparing two groups and one-way analysis of variance (ANOVA) followed by Tukey's posthoc analysis for comparing three or more groups.

REPRESENTATIVE RESULTS:

Following the successful implementation of the above protocol, representative results are shown for a typical styryl dye synaptic vesicle release experiment. Cultured rat primary cortical neurons were loaded with dye using the method described in section 6. The specificity of dye loading was determined by co-labeling with synaptic vesicle marker synaptophysin. A majority of styryl dye positive puncta are co-positive for this marker (**Figure 2A**). To determine whether the settings used for styryl dye imaging cause photobleaching, typically, an untreated well is loaded with dye and imaged for an extended 10 min period without stimulation to make sure fluorescence values remain constant.

Additionally, results are again shown using co-labeling of synaptophysin and styryl dye as in **Figure 2A**. These fluorophores were co-imaged using the paradigm indicated in section 6 for TRITC styryl dye imaging, plus dual capture of synaptophysin fluorescence using high-intensity laser power on the DAPI channel to visualize the mTurquoise-synaptophysin. Shown are representative images of synaptic regions pre- and post-stimulation (**Figure 2B**). While this method is an indirect inference for lack of photobleaching, analysis of the raw intensity values over the entire imaging period reveals that synaptophysin intensity remains constant, while styryl dye intensity goes down following stimulation (**Figure 2C**). Thus, taking this experiment and our other controls of stable fluorescence before stimulation and over extended periods in non-

stimulation wells, we have established that decreases in styryl fluorescence can be attributed to synaptic unloading through KCl depolarization rather than photobleaching effects.

[Place Figure 2 here]

Representative images show the loading of styryl dye during imaging, with the selection of ROIs (**Figure 3A–B**). The raw fluorescence intensity of selected ROIs and a background ROI are plotted using the confocal software (**Figure 3C**). The neurons shown here were also transfected with plasmids to study the effects of dipeptide proteins produced in the context of C9ORF72-ALS, namely, FLAG-eGFP and FLAG-GA₅₀-eGFP driven off of the T7 promoter. Successful synaptic vesicle release results in striking loss of dye fluorescence upon high KCl depolarization (**Figure 3D, top two panels**) for a GFP-transfected control neuron. A representative video included here demonstrates how this appears during imaging. In addition, a neuron selectively unloads styryl dye in a neurite region following stimulation (**Video 1**).

On the other hand, impaired synaptic transmission is represented by retained dye fluorescence even after high KCl depolarization in neurons transfected with a C9ORF72-linked dipeptide repeat construct (GA₅₀) (**Figure 3D, bottom two panels**)⁴³. Following quantitative data analysis (**Figure 3E**), data are represented as dye intensity throughout imaging for the control (GFP) and ALS/FTD (GA₅₀) groups (**Figure 3F**)⁴³. This method can also parse intermediate effects and is not simply an "all or nothing" binary measure. In experiments designed to rescue the synaptic deficits mediated by GA₅₀, exogenous synaptic vesicle-associated protein 2 (SV2) was introduced by lentiviral transduction using the rSV2a-eGFP-pRRRL plasmid driven off of the human PGK promoter. Following imaging and analysis as outlined above, synaptic firing was rescued in neurons co-expressing GA₅₀ and SV2 (**Figure 3G**).

[Place Figure 3 here]

[Place Video 1 here]

Following the method described in section 7, shown are representative fluorescence images of cortical neurons transfected with GcaMP6m before and after KCl depolarization (**Figure 4A**). Raw intensity graphs show increased fluorescence values that fluctuate, indicating calcium entry into neurites following KCl-induced depolarization (**Figure 4B**). This second representative video shows neurons expressing GcaMP6m with low fluorescence at the end of the recording baseline period to demonstrate this effect. At the start of the stimulation, the neurons display a dramatic fluorescence increase (**Video 2**). This approach has been successfully utilized to demonstrate calcium-entry alterations in a mutant FUS-ALS model. Astrocytes in this model were transduced with adenovirus containing CMV-promoter-driven eGFP-FUS plasmids. When conditioned medium from mutant FUS-expressing astrocytes was placed on motor neurons, increased calcium influx was observed compared to non-mutant FUS conditions following depolarization (**Figure 4C**)⁴⁴. The sensitivity of this assay have been tested by performing experiments with and without calcium included in the perfusion medium. In the setting of GFP versus GA₅₀ mentioned above, increased peak calcium transients was observed in GA₅₀ containing motor neurons.

Notably, this depended on calcium coming into the cell and not the release of internal calcium stores. When calcium was removed from the stimulating aCSF medium, no calcium transient responses were noted in either experimental condition (**Figure 4D**)⁴³.

[Place Figure 4 here]

[Place Video 2 here]

FIGURE AND TABLE LEGENDS:

Figure 1: Visual rendering of overall general protocol process. (1) Isolate and culture primary rodent neurons *in vitro* to chosen maturation timepoint. (2) Introduce GCaMP DNA or styryl dye as reporters of synaptic activity. (3) Setup imaging paradigm using live-imaging equipped confocal microscope and associated software. Begin baseline recording period. (4) While cells are still undergoing live-image capture, stimulate neurons via high KCl bath perfusion. (5) Assess fluorescence intensity measurements over time to measure calcium transients or synaptic vesicle fusion.

Figure 2: Assessment of specificity and imaging parameters of styryl dye labeling. (A) A representative 40x image of a styryl dye-labeled rat cortical neuron (red), which was transfected 24 h previously with a plasmid to express mTurquoise2-synaptophysin⁶¹ driven off the synapsin promoter (green). Colocalization of these two fluorophores indicates that a large majority of styryl dye positive puncta are co-stained with synaptic vesicle marker synaptophysin. Scale bar indicates 5 μm . (B) Cortical neurons were transfected and styryl dye loaded as in (A) and imaged according to the styryl dye paradigm along with dual fluorescence capture of the mTurquoise-synaptophysin on the DAPI channel. Representative images are showing synaptophysin and styryl dye puncta regions pre- and post-stimulation. Scale bar indicates 5 μm . (C) Fluorescence was monitored over time for synaptophysin (DAPI channel top) and styryl dye (FITC channel bottom). Synaptophysin intensity was maintained at a steady fluorescence over the imaging and stimulation period, while styryl dye fluorescence decreased as the dye was unloaded at stimulation.

Figure 3: Evaluating synaptic vesicle release through styryl dye labeling. (A) A representative 40x image of a styryl dye-labeled neuron in low KCl aCSF media at the start of an imaging experiment. Scale bar indicates 20 μm . (B) Depiction of ROI generation on the image from (A). Specific puncta regions along neurites (#1–4) are chosen using the ROI tool, the bean-shaped button highlighted at the right. A final ROI (#5) is selected in a blank region to capture background signal intensity. Areas with non-specific, non-neuronal bright spots are avoided. Scale bar indicates 20 μm . (C) Representation of the signal intensities for ROIs #1–5 from (B) over time as graphed/depicted by confocal software. (D) Visual representations of ROI regions pre/post-stimulation for a neuron that effectively undergoes synaptic transmission (top two panels). The bottom two panels are zoomed images with an unbiased threshold applied to isolate puncta from the background to show distinct regions visually. GFP-containing neurons effectively undergo synaptic release, whereas expression of C9ORF2-ALS related peptide GA₅₀ prevents this effect. Scale bars indicate 10 μm —Reprinted from Jensen et al. 2020⁴³. (E) Example of a quantification

file using spreadsheet software, showing normalization of values to baseline and generation of $\Delta F/F$ values over time. Data are first normalized to the background ROI intensity value at each time point. This value is then compared to the average ROI of interest baseline value for the last 30 s pre-stimulation (shown here as 10 s in 1 s intervals for simplicity) (ΔF). This change is next calculated as a fraction of the baseline fluorescence ($\Delta F/F$). Finally, the starting point value is set to 1 so that increases or decreases can be easily visualized graphically over time. At least five puncta regions per neuron and at least ten neurons per experimental condition are collected, with data such as this combined to generate average measurements at each time point. (F) Data from a spreadsheet file such as in (E) are moved into a graphing and statistics software program. For the graph shown here, the $\Delta F/F$ value at each timepoint averaged over all puncta regions of an experimental condition is plotted, along with its standard error of the mean. The graph here is data from the GFP versus GA₅₀ experiments indicated in (D), where the last 10 s of baseline and first 10 s of the stimulation period are shown—reprinted from Jensen et al. 2020⁴³. (G) This assay can produce curves for intermediate synaptic release and is not simply an "all or nothing" response. GA₅₀ was co-expressed with exogenous synaptic protein SV2 (synaptic vesicle-associated protein 2), and styryl dye imaging and analysis were performed as indicated in the previous steps. As in **Figure 3F**, the graph shown here represents the $\Delta F/F$ value at each timepoint averaged over all puncta regions of an experimental condition is plotted, along with its standard error of the mean. The graph shows the last minute of baseline and the first minute of the stimulation period from Jensen et al. 2020⁴³.

Figure 4: Observing calcium transients in real-time using GCaMP reporters. (A) A 40x image of a GCaMP6m expressing neuron, pseudo-colored to show the intensity of GFP fluorescence (low in blue to high in red). Left-hand panels show the whole 40x field of view pre- and post-stimulation. Scale bar indicates 20 μ m. The images to the right are zoomed versions of the boxed areas revealed. Through these images, it is evident by eye that there is a robust increase in focal neuritic calcium levels following stimulation. Scale bar indicates 12 μ m. (B) ROI selection and fluorescence intensity monitoring throughout the experiment is performed as in **Figure 3**. The final 30 s of baseline and 1 min stimulation for two selected ROIs of a neuron undergoing GCaMP6m fluorescence monitoring is shown here. In contrast to styryl dye imaging, the fluorescence intensity increases following neuronal stimulation. Additionally, as is noted here, calcium transients fluctuate in neurites over time; therefore, results are typically represented as the averaged peak normalized fluorescence change value for each ROI region. (C) Representative quantification of such an experiment is shown as was published in Kia-McAvoy et al. 2018⁴⁴, where supernatant derived from mutant FUS-ALS astrocytes caused a significantly increased influx of calcium in primary rodent motor neurons than supernatant from wild-type FUS expressing astrocytes. (D) Representative quantification of calcium transient imaging where calcium was not included in the stimulating aCSF. Shown are conditions of mCherry versus GA₅₀-mCherry stimulated with high KCl aCSF with or without calcium as published in Jensen et al. 2020⁴³. GA₅₀ containing neurons displayed increased peak calcium influx compared with mCherry containing cells. There was no elevation of internal calcium levels in either experimental condition when calcium was removed from stimulating high KCL aCSF.

Table 1: Composition of artificial cerebrospinal fluid (aCSF) buffers. This table includes the ingredients for preparing low and high KCl artificial cerebrospinal fluid buffers used while imaging and stimulating neurons. See section 4 for preparation instructions.

Table 2: Possible problems and troubleshooting for styryl dye experiments. Typical scenarios for issues and general troubleshooting for synaptic unloading experiments.

Table 3: Possible problems and troubleshooting for imaging calcium transients in neurites. Typical scenarios for issues and general troubleshooting for GCaMP calcium transient experiments.

Video 1: Representative video of styryl dye imaging experiment. Shown is a representative video of a cortical neuron loaded with styryl dye. The video shows the period beginning at the time of bath perfusion of high KCl aCSF. The boxed region highlights the neurites, with observable loss of puncta fluorescence over time.

Video 2: Representative video of GCaMP calcium transient experiment. Shown is a representative video of a field of cortical neurons transfected with GCaMP6m. Following a baseline period, a large calcium influx is noted at the 6 s mark when high KCl aCSF was applied. Calcium entry can be measured either for the whole cell, or at specific neurite regions as described.

DISCUSSION:

Three steps common to both methods described are of crucial importance for experimental success and quantifiable outcomes. First, preparation of fresh aCSF before each round of experiments is essential, following the attached instructions. Failure to do so may prevent appropriate neuronal depolarization. A sample of untreated control neurons should constantly be tested before stimulation of any experimental groups to ensure proper cellular depolarization and provide a benchmark for positive results obtained in that imaging session. Second, to successfully track fluorescence over time for specific synaptic regions, particular care should also be taken when setting up imaging parameters and areas of ROIs for monitoring. The baseline period recording should immediately transition to the stimulation recording period. A sufficiently rapid frame rate (2 images/s) is required to capture the single-decay dynamics of styryl dye release. Finally, a critical step in the analysis of experimentation is the normalization of fluorescence measurements first to the imaging background and then to the pre-stimulated baseline. As with other imaging protocols, subtraction of a blank imaging region is first performed across all paired time-fluorescence measurements to remove any artifactual fluorescence that the addition of KCl media may introduce. It is also essential to measure and calculate the average fluorescence reading for each ROI from the last 30 s baseline before stimulation. This average starting value is then used across all time measurements for that ROI as a defined starting point to quantify the "change from baseline" intensity.

Primary neuronal culture is notoriously difficult to transfect with exogenous DNA, and even optimized protocols frequently yield low efficiencies of total cells in culture. 20%–25% of

transfection efficiency is commonly achieved in our neuronal cultures, with no evidence of transfection-induced toxicity. While fairly consistent expressions are seen across cells containing GCaMP, subtly differing levels of probe expression within individual cells are considered based on the method of individual region quantification of change in baseline fluorescence compared to that baseline. However, with this relatively low efficiency, using transfection-based methods of introducing the GCaMP reporter is not of sufficient robustness for large-scale biological replicates for high throughput screening studies. To overcome this, several variant constructs are commercially available for lentiviral or adenoviral packaging or cell-lineage specific expression, which will allow for higher transduction efficiencies. A primary modification that may be desired when using these protocols is to use optogenetic stimulation of neurons instead of bath application of KCl⁶². Transduction with lentiviral constructs designed to express one of the families of now available channelrhodopsins, followed by activation with specific wavelengths of light, allows for spatial control for depolarization of subsets of neurons and also for the evaluation of the effect of trains of action potentials on repetitive calcium influx levels and depletion of synaptic vesicle stores⁶³. However, it is essential to keep in mind that usage of this method is presently somewhat constrained, as the user must ensure that their optogenetic reporter, synaptic reporter, and any additional exogenously introduced proteins do not have spectral overlap between utilized fluorophores. A common troubleshooting issue using the styryl dye is passive intensity reduction during the baseline recording period. Before experimental studies, it is critical to optimize laser intensity and photo capture intervals to minimize photobleaching effects. For experiments to be considered, stabilization of intensity for at least the last 30 s of the baseline period is necessary. Refer to **Tables 2** and **Table 3** for common problems and their solutions for styryl dye and calcium transient experiments, respectively.

The primary limitation of these two methods is that cultures can only be stimulated and examined in a single instance. As bath application is used to introduce the depolarizing agent KCl, all neurons to be examined from that condition in that dish must be within the initial field of view of the microscope objective. If functionality over time is of interest, paired cultures are required. However, the optogenetic method mentioned above will allow calcium dynamics to be observed over time if desired. Additionally, if neurons have a defect in the recycling of synaptic vesicles, the initial loading of the styryl dye will be impaired. While internal intensity normalization allows for comparison across conditions, slight differences in magnitudes of responses may be difficult to detect. Finally, new iterations of these reporters have rapidly become available and can be switched out for faster detection times or more robust results. For example, GCaMP6m is no longer considered the quickest reporter of calcium transients at synaptic terminals. Instead, one can utilize the latest generation jGCaMP8⁶⁴.

The methods described here are a fast and reliable way to determine whether genetic or pharmacological manipulation of neurons perturbs functional synaptic signaling and release. The detailed experiments are less technically challenging and less costly than traditional voltage/current clamp electrophysiology and electron microscopy. Additionally, while electrophysiology is by nature low throughput and on the individual cell level, the protocols here described are higher throughput and rapid, allowing several neurons to be imaged simultaneously and many iterations to be performed in a single imaging session. It is proposed

that these calcium dynamics and synaptic release paradigms be used as the first indicator of synaptic transmission alterations in ALS models and the study of other forms of neuronal degeneration. Although the conclusions derived from Gcamp6m and styryl dye imaging cannot precisely tease out a specific mechanism of synaptic dysfunction, based on such findings, researchers can then undertake targeted, evidence-based complementary studies using traditional methods to determine channels involved, synaptic vesicle number, or quantal content.

The utility in these protocols is the rapid and straightforward assessment of alterations in proper depolarization-mediated calcium influx and/or synaptic vesicle fusion in specific ALS models. We have recently demonstrated this in a publication showing increased calcium influx and abrogation of synaptic unloading in cortical neurons expressing the dipeptide protein (glycine-alanine)₅₀ resulting from the C9ORF72 hexanucleotide repeat expansion⁴³. As shown in our published work, these methods can be performed easily in tandem with co-transfection of mutant RNAs or proteins of interest or in cells cultured directly from transgenic animal models⁴³. Additionally, the reliability and robustness of these protocols have successfully tested in neuronally-differentiated human induced pluripotent stem cells⁴⁵, enabling future studies to be done directly in patient-derived disease-relevant cells. In another recent manuscript, we provide evidence that wild-type motor neurons undergo high calcium influx following stimulation when in the presence of a soluble factor released from mutant FUS expressing astrocytes⁴⁴. Astrocytic calcium signaling events are also deeply intertwined with the synaptic transmission in neighboring neurons⁶⁵. Calcium dynamics protocol have been applied to investigate whole-cell calcium transients in models of astrocytic culture, which has proven effective in both rodents primary and human IPS-derived cells. Further understanding of astrocytic calcium dynamics and signaling in ALS models will provide valuable insight into how synaptic transmission maybe consequently affected. Ultimately, employing cell-type-specific GCaMP reporters will also be a powerful tool for investigating neuronal and astrocytic calcium dynamics in mixed co-culture settings and specifically evaluating non-cell-autonomous effects originating from each cell population.

Finally, the potential usage of these methods extends not just beyond the study of ALS, but also to the broader fields of neurodegenerative and even developmental neuroscience. Detailed information about the specific plasmids used to generate the representative results is provided and successful at transfecting plasmids containing many different genetic variants of FUS, SOD1 and C9ORF72 hexanucleotide repeats and dipeptides^{43,44,66–68}. Provided that plasmids contain a promoter used in neurons, there is no limitation on what models of ALS or degenerative disease could be studied using these methods. Furthermore, transfection to express mutant proteins is an entirely optional step. Cultures generated from transgenic animals or human patient-derived cells eliminate the need to identify cells containing the mutant protein of interest. Presently, these systems are constrained in the fashion that if styryl dye will be used, the TRITC channel is occupied, and if GcaMP6 is used, the FITC channel is occupied. Techniques that allow for the examination of neuronal and astrocytic activity in real-time broaden the possibilities for understanding time-course analysis for synaptic maturation/degeneration, as well as rapid tests for the efficacy of pharmacological compounds in promoting or suppressing neuronal communication. These two methods are amenable to high throughput scaling for screening.

Rather than plating neurons in individual 35 mm dishes, the imaging parameters of these two protocols could be employed in an automated fashion across 96-well plates. Using such a platform, compound libraries can be quickly tested for therapeutics, which modulate calcium entry or improve synaptic release using a genetic model of disease or even cells derived directly from patients. This method could fast-track the possibility of subgroup-specific or even personalized therapeutics by rapidly identifying candidate molecules for further investigation.

ACKNOWLEDGMENTS:

We would like to acknowledge the present and former members of the Jefferson Weinberg ALS Center for critical feedback and suggestions for optimizing these techniques and their analyses. This work was supported by funding from the NIH (RF1-AG057882-01 and R21-NS0103118 to D.T.), the NINDS (R56-NS092572 and R01-NS109150 to P.P.), the Muscular Dystrophy Association (D.T.), the Robert Packard Center for ALS Research (D.T.), the Family Strong 4 ALS foundation and the Farber Family Foundation (B.K.J., K.K, and P.P).

DISCLOSURES:

The authors declare that they have no conflicts of interest.

REFERENCES:

1. Gibson, S. B. et al. The evolving genetic risk for sporadic ALS. *Neurology*. **89** (3), 226–233 (2017).
2. Kim, G., Gautier, O., Tassoni-Tsuchida, E., Ma, X. R., Gitler, A. D. ALS genetics: Gains, losses, and implications for future therapies. *Neuron*. **108** (5), 822–842 (2020).
3. Nijssen, J., Comley, L. H., Hedlund, E. Motor neuron vulnerability and resistance in amyotrophic lateral sclerosis. *Acta Neuropathologica*. **133** (6), 863–885 (2017).
4. Marttinen, M., Kurkinen, K. M., Soininen, H., Haapasalo, A., Hiltunen, M. Synaptic dysfunction and septin protein family members in neurodegenerative diseases. *Molecular Neurodegeneration*. **10**, 16 (2015).
5. Bae, J. S., Simon, N. G., Menon, P., Vucic, S., Kiernan, M. C. The puzzling case of hyperexcitability in amyotrophic lateral sclerosis. *Journal of Clinical Neurology*. **9** (2), 65–74 (2013).
6. Kiernan, M. C. Hyperexcitability, persistent Na⁺ conductances and neurodegeneration in amyotrophic lateral sclerosis. *Experimental Neurology*. **218** (1), 1–4 (2009).
7. Krarup, C. Lower motor neuron involvement examined by quantitative electromyography in amyotrophic lateral sclerosis. *Clinical Neurophysiology*. **122** (2), 414–422 (2011).
8. Vucic, S., Nicholson, G. A., Kiernan, M. C. Cortical hyperexcitability may precede the onset of familial amyotrophic lateral sclerosis. *Brain*. **131** (Pt 6), 1540–1550 (2008).
9. Marchand-Pauvert, V. et al. Absence of hyperexcitability of spinal motoneurons in patients with amyotrophic lateral sclerosis. *Journal of Physiology*. **597** (22), 5445–5467 (2019).
10. Fischer, L. R. et al. Amyotrophic lateral sclerosis is a distal axonopathy: evidence in mice and man. *Experimental Neurology*. **185** (2), 232–240 (2004).
11. Markert, S. M. et al. Overexpression of an ALS-associated FUS mutation in *C. elegans* disrupts NMJ morphology and leads to defective neuromuscular transmission. *Biology Open*. **9** (12) (2020).

- 834 12. Shahidullah, M. et al. Defects in synapse structure and function precede motor neuron
835 degeneration in Drosophila models of FUS-related ALS. *Journal of Neuroscience*. **33** (50), 19590–
836 19598 (2013).
- 837 13. Liu, Y. et al. C9orf72 BAC Mouse Model with Motor Deficits and Neurodegenerative
838 Features of ALS/FTD. *Neuron*. **90** (3), 521–534 (2016).
- 839 14. Freibaum, B. D. et al. GGGGCC repeat expansion in C9orf72 compromises
840 nucleocytoplasmic transport. *Nature*. **525** (7567), 129–133 (2015).
- 841 15. Zhang, K. et al. The C9orf72 repeat expansion disrupts nucleocytoplasmic transport.
842 *Nature*. **525** (7567), 56–61 (2015).
- 843 16. Perry, S., Han, Y., Das, A., Dickman, D. Homeostatic plasticity can be induced and
844 expressed to restore synaptic strength at neuromuscular junctions undergoing ALS-related
845 degeneration. *Human Molecular Genetics*. **26** (21), 4153–4167 (2017).
- 846 17. Romano, G. et al. Chronological requirements of TDP-43 function in synaptic organization
847 and locomotive control. *Neurobiology of Disease*. **71**, 95–109 (2014).
- 848 18. Armstrong, G. A., Drapeau, P. Calcium channel agonists protect against neuromuscular
849 dysfunction in a genetic model of TDP-43 mutation in ALS. *Journal of Neuroscience*. **33** (4), 1741–
850 1752 (2013).
- 851 19. Diaper, D. C. et al. Loss and gain of Drosophila TDP-43 impair synaptic efficacy and motor
852 control leading to age-related neurodegeneration by loss-of-function phenotypes. *Human*
853 *Molecular Genetics*. **22** (8), 1539–1557 (2013).
- 854 20. Schwiening, C. J. A brief historical perspective: Hodgkin and Huxley. *Journal of Physiology*.
855 **590** (11), 2571–2575 (2012).
- 856 21. Dong, H. et al. Curcumin abolishes mutant TDP-43 induced excitability in a motoneuron-
857 like cellular model of ALS. *Neuroscience*. **272**, 141–153 (2014).
- 858 22. Chand, K. K. et al. Defects in synaptic transmission at the neuromuscular junction precede
859 motor deficits in a TDP-43(Q331K) transgenic mouse model of amyotrophic lateral sclerosis.
860 *Federation of American Societies for Experimental Biology Journal*. **32** (5), 2676–2689 (2018).
- 861 23. Perkins, E. M. et al. Altered network properties in C9ORF72 repeat expansion cortical
862 neurons are due to synaptic dysfunction. *Molecular Neurodegeneration*. **16** (1), 13 (2021).
- 863 24. Ceccarelli, B., Hurlbut, W. P. Vesicle hypothesis of the release of quanta of acetylcholine.
864 *Physiological Reviews*. **60** (2), 396–441 (1980).
- 865 25. Ettinger, A., Wittmann, T. Fluorescence live cell imaging. *Methods in Cell Biology*. **123**, 77–
866 94 (2014).
- 867 26. Ryan, J., Gerhold, A. R., Boudreau, V., Smith, L., Maddox, P. S. Introduction to Modern
868 Methods in Light Microscopy. *Methods in Molecular Biology*. **1563**, 1–15 (2017).
- 869 27. Wang, L., Frei, M. S., Salim, A., Johnsson, K. Small-molecule fluorescent probes for live-
870 cell super-resolution microscopy. *Journal of the American Chemical Society*. **141** (7), 2770–2781
871 (2019).
- 872 28. Neher, E. Vesicle pools and Ca²⁺ microdomains: new tools for understanding their roles
873 in neurotransmitter release. *Neuron*. **20** (3), 389–399 (1998).
- 874 29. Dolphin, A. C., Lee, A. Presynaptic calcium channels: specialized control of synaptic
875 neurotransmitter release. *Nature Reviews Neuroscience*. **21** (4), 213–229 (2020).
- 876 30. Tsien, R. Y., Rink, T. J., Poenie, M. Measurement of cytosolic free Ca²⁺ in individual small
877 cells using fluorescence microscopy with dual excitation wavelengths. *Cell Calcium*. **6** (1–2), 145–

157 (1985).

31. Takahashi, N. et al. Cytosolic Ca²⁺ dynamics in hamster ascending thin limb of Henle's loop. *American Journal of Physiology*. **268** (6 Pt 2), F1148–1153 (1995).

32. Cleemann, L., DiMassa, G., Morad, M. Ca²⁺ sparks within 200 nm of the sarcolemma of rat ventricular cells: evidence from total internal reflection fluorescence microscopy. *Advances in Experimental Medicine and Biology*. **430**, 57–65 (1997).

33. Roe, M. W., Lemasters, J. J., Herman, B. Assessment of Fura-2 for measurements of cytosolic free calcium. *Cell Calcium*. **11** (2–3), 63–73 (1990).

34. Lin, M. Z., Schnitzer, M. J. Genetically encoded indicators of neuronal activity. *Nature Neuroscience*. **19** (9), 1142–1153 (2016).

35. Tian, L. et al. Imaging neural activity in worms, flies and mice with improved GCaMP calcium indicators. *Nature Methods*. **6** (12), 875–881 (2009).

36. Nakai, J., Ohkura, M., Imoto, K. A high signal-to-noise Ca(2+) probe composed of a single green fluorescent protein. *Nature Biotechnology*. **19** (2), 137–141 (2001).

37. Chen, T. W. et al. Ultrasensitive fluorescent proteins for imaging neuronal activity. *Nature*. **499** (7458), 295–300 (2013).

38. Horikawa, K. Recent progress in the development of genetically encoded Ca²⁺ indicators. *Journal of Medical Investigation*. **62** (1–2), 24–28 (2015).

39. Bohme, M. A., Grasskamp, A. T., Walter, A. M. Regulation of synaptic release-site Ca(2+) channel coupling as a mechanism to control release probability and short-term plasticity. *Federation of European Biochemical Society Letters*. **592** (21), 3516–3531 (2018).

40. Li, Y. C., Kavalali, E. T. Synaptic vesicle-recycling machinery components as potential therapeutic targets. *Pharmacological Reviews*. **69** (2), 141–160 (2017).

41. Gaffield, M. A., Betz, W. J. Imaging synaptic vesicle exocytosis and endocytosis with FM dyes. *Nature Protocols*. **1** (6), 2916–2921 (2006).

42. Verstreken, P., Ohyama, T., Bellen, H. J. FM 1-43 labeling of synaptic vesicle pools at the *Drosophila* neuromuscular junction. *Methods in Molecular Biology*. **440**, 349–369 (2008).

43. Jensen, B. K. et al. Synaptic dysfunction induced by glycine-alanine dipeptides in C9orf72-ALS/FTD is rescued by SV2 replenishment. *European Molecular Biology Organization Molecular Medicine*. **12** (5), e10722 (2020).

44. Kia, A., McAvoy, K., Krishnamurthy, K., Trotti, D., Pasinelli, P. Astrocytes expressing ALS-linked mutant FUS induce motor neuron death through release of tumor necrosis factor- α . *Glia*. **66** (5), 1016–1033 (2018).

45. Fernandopulle, M. S. et al. Transcription Factor-Mediated Differentiation of Human iPSCs into Neurons. *Current Protocols in Cell Biology*. **79** (1), e51 (2018).

46. Ye, L., Haroon, M. A., Salinas, A., Paukert, M. Comparison of GCaMP3 and GCaMP6f for studying astrocyte Ca²⁺ dynamics in the awake mouse brain. *Public Library of Science One*. **12** (7), e0181113 (2017).

47. Angleson, J. K., Betz, W. J. Monitoring secretion in real time: capacitance, amperometry and fluorescence compared. *Trends in Neuroscience*. **20** (7), 281–287 (1997).

48. Ryan, T. A. et al. The kinetics of synaptic vesicle recycling measured at single presynaptic boutons. *Neuron*. **11** (4), 713–724 (1993).

49. Kraszewski, K. et al. Synaptic vesicle dynamics in living cultured hippocampal neurons visualized with CY3-conjugated antibodies directed against the luminal domain of

synaptotagmin. *Journal of Neuroscience*. **15** (6), 4328–4342 (1995).

50. Betz, W. J., Mao, F., Bewick, G. S. Activity-dependent fluorescent staining and destaining of living vertebrate motor nerve terminals. *Journal of Neuroscience*. **12** (2), 363–375 (1992).

51. Betz, W. J., Bewick, G. S. Optical analysis of synaptic vesicle recycling at the frog neuromuscular junction. *Science*. **255** (5041), 200–203 (1992).

52. Ryan, T. A., Smith, S. J. Vesicle pool mobilization during action potential firing at hippocampal synapses. *Neuron*. **14** (5), 983–989 (1995).

53. Betz, W. J., Ridge, R. M., Bewick, G. S. Comparison of FM1-43 staining patterns and electrophysiological measures of transmitter release at the frog neuromuscular junction. *Journal of Physiology-Paris*. **87** (3), 193–202 (1993).

54. Wu, L. G., Betz, W. J. Nerve activity but not intracellular calcium determines the time course of endocytosis at the frog neuromuscular junction. *Neuron*. **17** (4), 769–779 (1996).

55. Ryan, T. A., Smith, S. J., Reuter, H. The timing of synaptic vesicle endocytosis. *Proceedings of the National Academy of Sciences of the United States of America*. **93** (11), 5567–5571 (1996).

56. Ramaswami, M., Krishnan, K. S., Kelly, R. B. Intermediates in synaptic vesicle recycling revealed by optical imaging of *Drosophila* neuromuscular junctions. *Neuron*. **13** (2), 363–375 (1994).

57. Kayser, M. S., McClelland, A. C., Hughes, E. G., Dalva, M. B. Intracellular and trans-synaptic regulation of glutamatergic synaptogenesis by EphB receptors. *Journal of Neuroscience*. **26** (47), 12152–12164 (2006).

58. Washburn, H. R., Xia, N. L., Zhou, W., Mao, Y. T., Dalva, M. B. Positive surface charge of GluN1 N-terminus mediates the direct interaction with EphB2 and NMDAR mobility. *Nature Communications*. **11** (1), 570 (2020).

59. Magrane, J., Sahawneh, M. A., Przedborski, S., Estevez, A. G., Manfredi, G. Mitochondrial dynamics and bioenergetic dysfunction is associated with synaptic alterations in mutant SOD1 motor neurons. *Journal of Neuroscience*. **32** (1), 229–242 (2012).

60. Casci, I. et al. Muscleblind acts as a modifier of FUS toxicity by modulating stress granule dynamics and SMN localization. *Nature Communications*. **10** (1), 5583 (2019).

61. Hruska, M., Henderson, N., Le Marchand, S. J., Jafri, H., Dalva, M. B. Synaptic nanomodules underlie the organization and plasticity of spine synapses. *Nature Neuroscience*. **21** (5), 671–682 (2018).

62. Rein, M. L., Deussing, J. M. The optogenetic (r)evolution. *Molecular Genetics and Genomics*. **287** (2), 95–109 (2012).

63. Bertucci, C., Koppes, R., Dumont, C., Koppes, A. Neural responses to electrical stimulation in 2D and 3D in vitro environments. *Brain Research Bulletin*. **152**, 265–284 (2019).

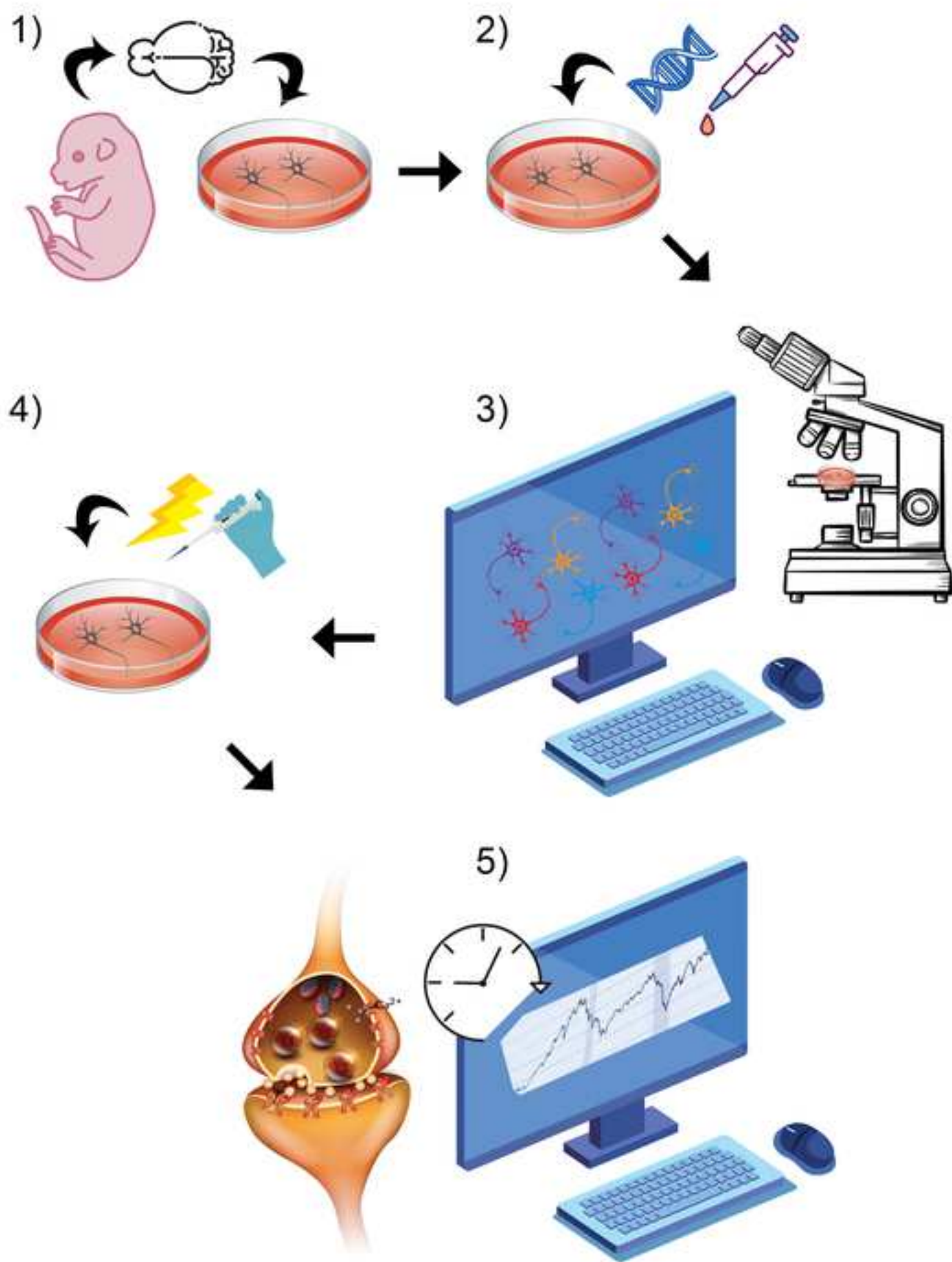
64. Zhang, Y. et al. jRCaMP1a Fast genetically encoded calcium indicators. *Janelia Research Campus* (2020).

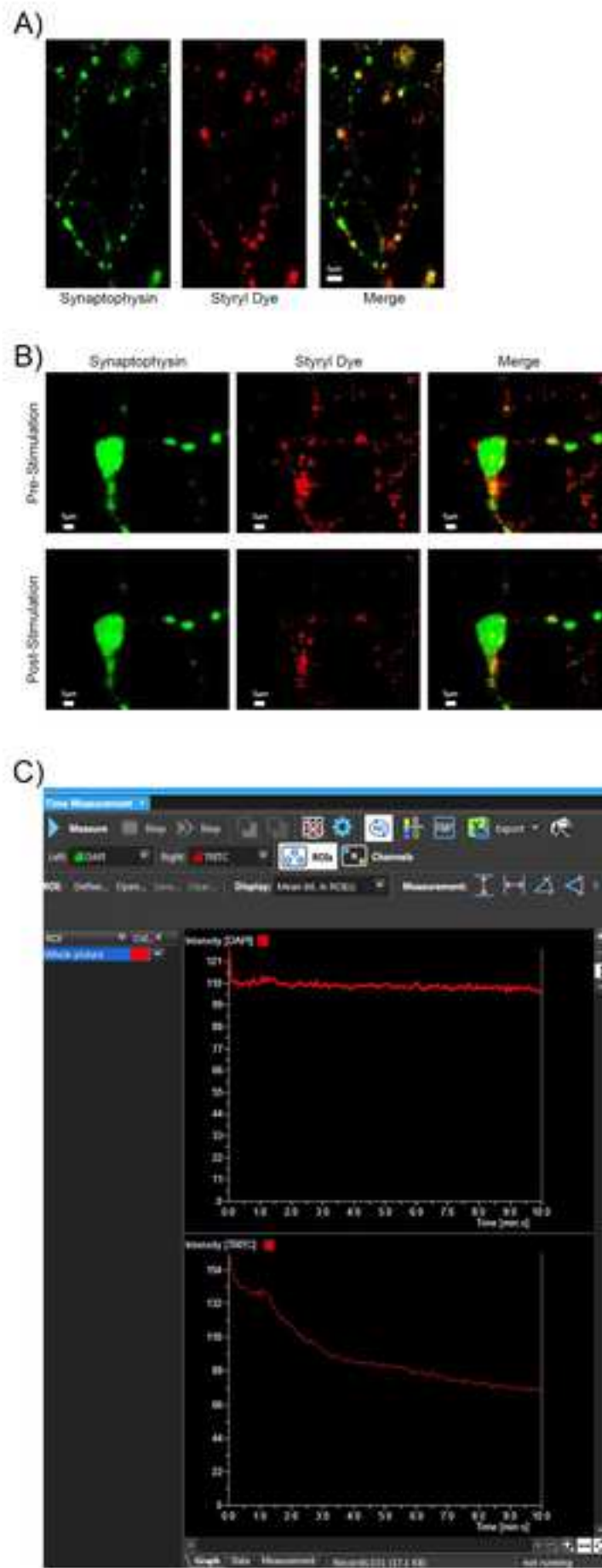
65. Guerra-Gomes, S., Sousa, N., Pinto, L., Oliveira, J. F. Functional roles of astrocyte calcium elevations: From synapses to behavior. *Frontiers in Cellular Neuroscience*. **11**, 427 (2017).

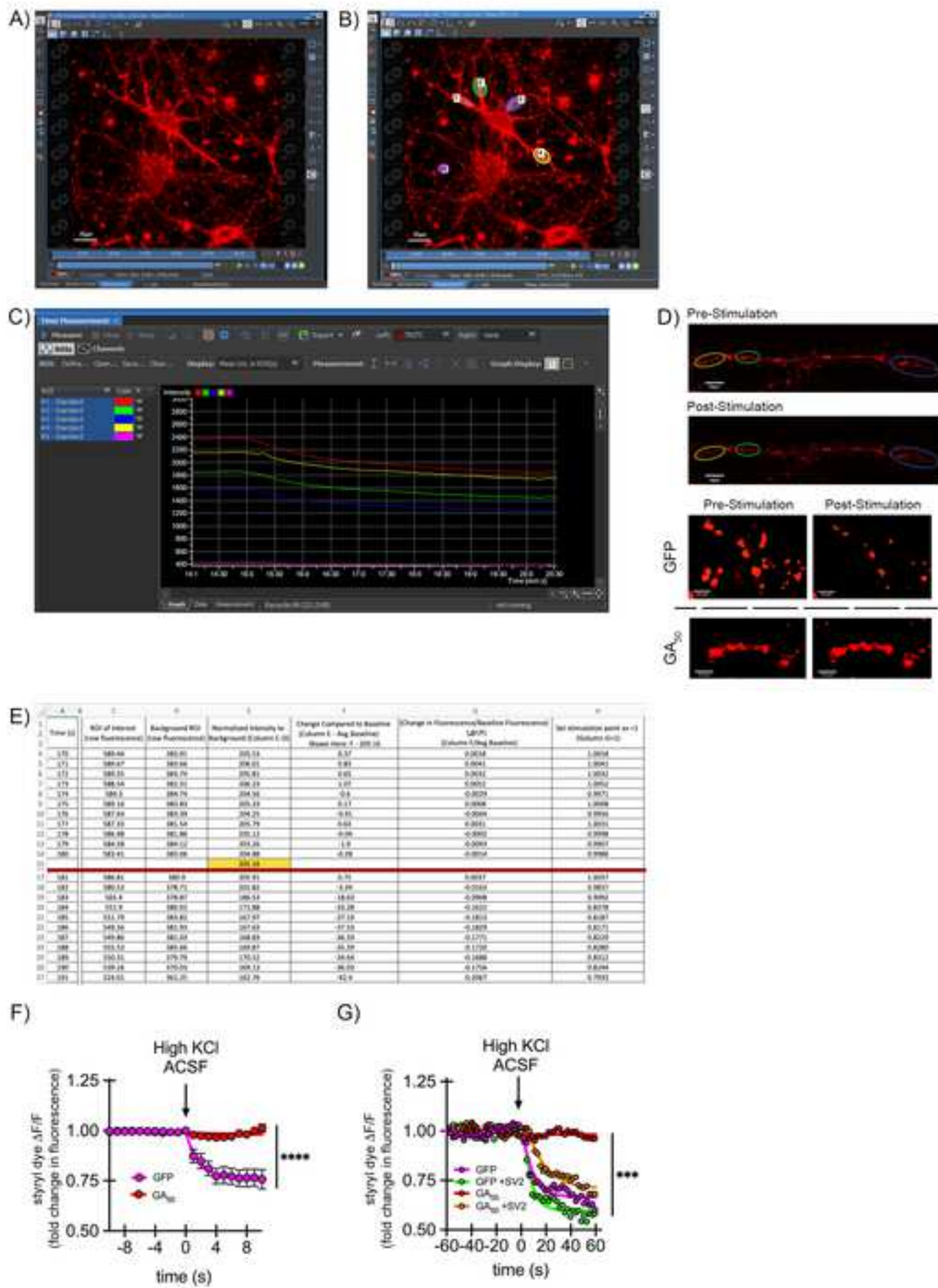
66. Westergaard, T. et al. Cell-to-cell transmission of dipeptide repeat proteins linked to C9orf72-ALS/FTD. *Cell Reports*. **17** (3), 645–652 (2016).

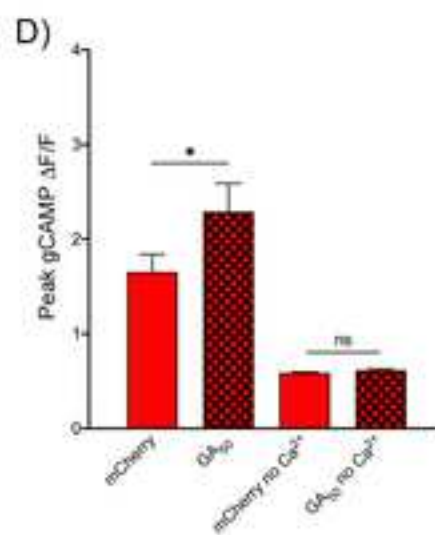
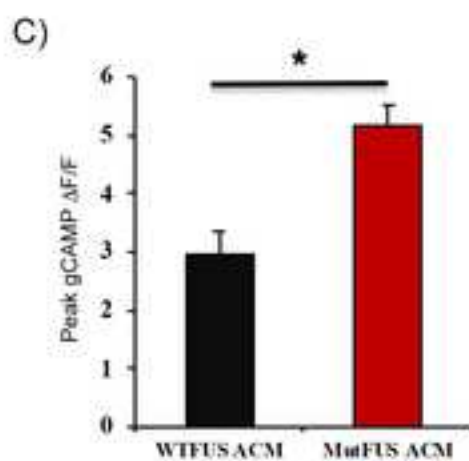
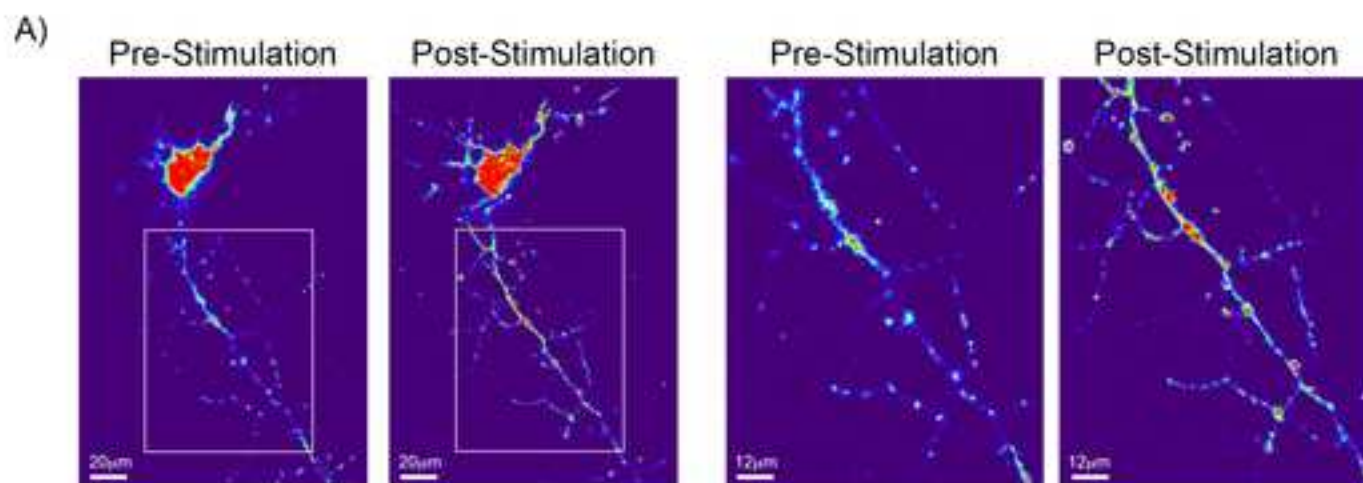
67. Wen, X. et al. Antisense proline-arginine RAN dipeptides linked to C9ORF72-ALS/FTD form toxic nuclear aggregates that initiate in vitro and in vivo neuronal death. *Neuron*. **84** (6), 1213–1225 (2014).

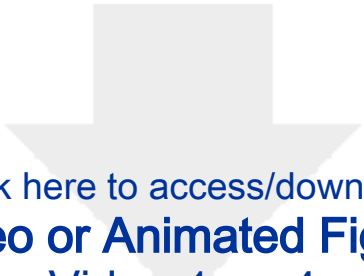
966 68. Daigle, J. G. et al. Pur-alpha regulates cytoplasmic stress granule dynamics and
967 ameliorates FUS toxicity. *Acta Neuropathologica*. **131** (4), 605–620 (2016).
968
969



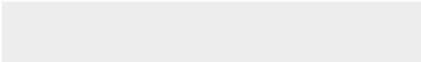



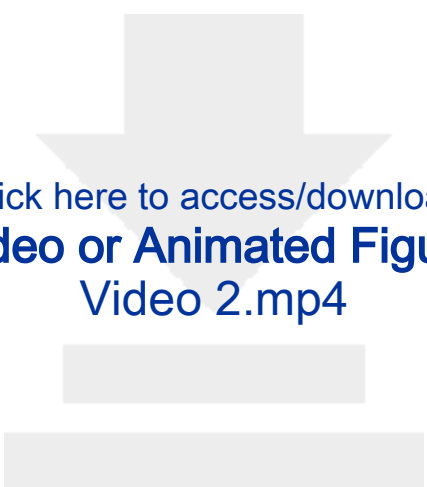






Click here to access/download
Video or Animated Figure
Video 1.mp4





Click here to access/download
Video or Animated Figure
Video 2.mp4

Composition of artificial cerebrospinal fluid (aCSF)

Low KCL aCSF buffer (pH 7.40 to 7.45)	
Reagent	Concentration
HEPES	10 mM
NaCl	140 mM
KCl	5 mM
Glucose	10 mM
CaCl ₂ 2H ₂ O	2 mM
MgCl ₂ 4H ₂ O	1 mM

High KCL aCSF buffer (pH 7.40 to 7.45)	
Reagent	Concentration
HEPES	10 mM
NaCl	95 mM
KCl	50 mM
Glucose	10 mM
CaCl ₂ 2H ₂ O	2 mM
MgCl ₂ 4H ₂ O	1 mM

	Potential problems
1	Non-specific loading
2	No appreciable exocytosis in control neurons
3	Loss of focus and lateral drift
4	Bleaching of FM4-64 fluorescence

Possible reasons/solution
Be precise with the loading time. Longer loading times result in non-specific loading of FM4-64 into endosomes and lysosomes
Check the pH of high KCl aCSF solution.
Make sure that perfect focus is on. Align the images post imaging using Nikon software or ImageJ plugin.
Check laser intensity used for imaging. Always try to use the lowest possible intensity. Confirm the laser intensity used does not result in bleaching by running trial runs.

	Potential problems	Possible reasons/solution
1	Transfection efficiency too low	Check neuronal health. If neurons are hard to transfect one can switch to AAV or lentiviral transduction of GCaMP.
2	Accumulation of GCaMP6 fluorescence in the nucleus	Compromised neuronal health. Check transfection protocol.
3	Loss of focus and lateral Image drift	Make sure that perfect focus is on. Align the images post imaging using Nikon software or ImageJ plugin.
4	No calcium response upon KCL stimulation	Make sure the pH of aCSF is correct.
5	Bleaching of GCaMP6 fluorescence	Check laser intensity used for imaging. Always try to use the lowest possible intensity. Confirm the laser intensity used does not result in bleaching by running trial runs.
6	Blebbing of neurites	Compromised neuronal health due to transfection. Use a fresh batch of neuronal cultures.



Click here to access/download

Table of Materials

Table of Materials.xls



We appreciate the substantial feedback from reviewers and have revised our manuscript accordingly. Thanks to the extensive review, there is no doubt that our manuscript has improved and we hope it will now be considered for publication with JoVE. Individual responses to each of the reviewer's comments can be found below.

Editorial comments:

Changes to be made by the Author(s):

1. Please take this opportunity to thoroughly proofread the manuscript to ensure that there are no spelling or grammar issues. Please define all abbreviations at first use.

[We have intently proofread the manuscript and appreciate the opportunity to do so.](#)

2. Please avoid abbreviations in the title and shorten it. Consider something along the lines of "Real-time fluorescent measurement of synaptic functions in models of amyotrophic lateral sclerosis."

[We have amended our title to shorten it according to this recommendation.](#)

3. Please revise the following lines to avoid overlap with previously published work: 108-112, 166-174.

[These sections have been substantially revised.](#)

4. JoVE cannot publish manuscripts containing commercial language. This includes trademark symbols (™), registered symbols (®), and company names before an instrument or reagent. Please remove all commercial language from your manuscript and use generic terms instead. All commercial products should be sufficiently referenced in the Table of Materials and Reagents.

[All commercial language has been removed from the main text, and is contained only within the Table of Materials and Reagents.](#)

5. Please revise the text, especially in the protocol, to avoid the use of any personal pronouns (e.g., "we", "you", "our" etc.).

[The use of personal pronouns has been removed from the protocol section and minimized elsewhere whenever possible.](#)

6. Being a video-based journal, JoVE authors must be very specific when it comes to humane treatment of animals. Regarding animal treatment in the protocol, please add the following information:

a) Please mention how the dams are anesthetized/euthanized to retrieve the embryos. If anesthetized, how proper anesthetization is confirmed. If euthanized, what was used (do not highlight these steps).

The following points are valid only in the case of anesthesia:

b) Please specify the use of vet ointment on eyes to prevent dryness while under anesthesia.

c) For survival strategies, discuss post-surgical treatment of animal, including recovery conditions and treatment for post-surgical pain.

d) Discuss maintenance of sterile conditions during survival surgery.

e) Please specify that the animal is not left unattended until it has regained sufficient consciousness to maintain sternal recumbency.

f) Please specify that the animal that has undergone surgery is not returned to the company of other animals until fully recovered.

[The pregnant rat dams were euthanized at the time of embryo collection. This has been explicitly stated in the protocol section with primary and secondary methods mentioned. No anesthesia was administered.](#)

7. Please ensure that all text in the protocol section is written in the imperative tense as if telling someone how to do the technique (e.g., "Do this," "Ensure that," etc.). The actions should be described in the imperative tense in complete sentences wherever possible. Avoid usage of phrases such as "could be," "should be," and "would be" throughout the Protocol. Any text that cannot be written in the imperative tense may be added as a "Note." However, notes should be concise and used sparingly. Please include all safety procedures and use of hoods, etc.

[The protocol section has been re-written in the imperative tense.](#)

8. Please note that your protocol will be used to generate the script for the video and must contain everything that you would like shown in the video. Please ensure you answer the “how” question, i.e., how is the step performed? Alternatively, add references to published material specifying how to perform the protocol action. There should be enough detail in each step to supplement the actions seen in the video so that viewers can easily replicate the protocol.

We have read through the protocol to ensure we have answered “how” each step is performed. Reviewer comments have also aided in guiding these revisions.

9. Please number your protocol steps as 1., 1.1., 1.1.1., 1.1.1.1. Please format the manuscript as: paragraph Indentation: 0 for both left and right and special: none, Line spacings: single. Please include a single line space between each step, substep and note in the protocol section. Please use Calibri 12 points and one-inch margins on all the side. Please include a one line space between each protocol step and then highlight UP TO 3 pages of protocol text for inclusion in the protocol section of the video. If your highlighting of a section heading means you want to film all the steps in that section, highlight all steps of relevant sections (not the notes/anesthesia/euthanasia) and ensure that the total length of highlighted text is three pages or less.

The formatting requested above has been completed. Appropriate portions of Sections 5-8 have been highlighted for filming.

10. Please include a scale bar for all images taken with a microscope to provide context to the magnification used. Define the scale in the appropriate Figure Legend.

All microscope images now have scale bars, with magnifications indicated in the corresponding figure legends.

11. Please ensure that the references appear as the following: [Lastname, F.I., LastName, F.I., LastName, F.I. Article Title. Source (ITALICS). Volume (BOLD) (Issue), FirstPage–LastPage (YEAR).] For 6 and more than 6 authors, list only the first author then et al. Please include volume and issue numbers for all references, and do not abbreviate the journal names. Ref 3 does not have any page numbers.

We have adjusted the reference section according to these specifications. It is worth noting, that the authors had downloaded the most recent JoVE Endnote library file for what we believed was proper formatting, and the presently available format style abbreviated journal names.

12. The Table of Materials need not have a legend of its own. It only needs to be referenced appropriately in the text (instead of commercial names). Hence, renumber the tables (2⇆1), (3⇆2), (4⇆3) and change the references in the text.

Thank you for this clarification. The associated legend has been removed, and other Tables have been renumbered.

Reviewers' comments:

Reviewer #1:

Manuscript Summary:

The manuscript titled "A live-cell imaging approach for real-time high throughput fluorescence measurement of synaptic function in models of ALS/FTD" by Jensen et al. describes a method to quantitatively assess vesicle excretion and Ca²⁺ fluctuations at synapses in culture. Each step of the protocol is described in detail, including primary neuronal cell preparation, transfection, experimental conditions, data requisition, and data analysis. A trouble shooting guide is also provided and limitations of this method are discussed.

Major Concerns:

I have no major concerns.

Minor Concerns:

The title is somewhat misleading as the authors do not describe a high throughput assay here - only an assays that is high throughput compatible.

We appreciate this feedback and have amended our title according to this suggestion as well as the editorial recommendation.

In the trouble shooting guide "issues" (sound colloquial) should be replaced with "potential problems.

This change has been made, and we agree that this sounds more professionally stated.

Also, I think the authors should de-emphasize the ALS aspect here as expression of ALS-associated proteins is merely used as a proof of principle here, whereas the describes method focuses on synaptic functions (vesicle excretion and Ca²⁺ transients). Therefore, the Discussion should extend on the possible applications of the method for ALS research but also so many other fields. Finally, the authors might want to add a section on how to make this method high throughput (e.g. as a perspective).

These final two comments have both been incorporated into our discussion section. We agree that while this invited review is intended for the publication "Current Models in ALS Research" that it has much broader application to anyone wishing to study synaptic functions. We have included details for the ALS-related plasmids and studies that we have performed, but have extended the discussion to better include other neurodegenerative and developmental fields. Additionally, we have now included more details on how these methods may be developed into high throughput screening assays, both for ALS and for other studies looking into modulating synaptic function.

Reviewer #2:

Manuscript Summary:

The manuscript describes about the couple of methods to assess activity of neurons using live imaging platform which are widely used and valuable for neuroscience research.

Major Concerns:

No major concerns

Minor Concerns:

1) Authors describe that they transfect cortical and motor neurons with the GCamp6s, Its would be useful to mention the transfection efficacy achieved by this method and comment on the viability of neurons upon transfection.

We appreciate this suggestion. Mention of these details is now included in the discussion section regarding transfection efficiency.

2) Details of how long the neurons are cultured needs to be provided.

Details of culturing time at which point synaptic function can be probed, along with when we perform our transfection and imaging experiments are now included.

2) Please provide details for plasmids used in the study, promoter etc.

These details have now been included.

3) Cell the specific expression of GCamp6 would be widely useful for complex co-culture experiments to assess non-cell autonomous effects in neurons, thus, I feel it would be useful to comment this in the discussion.

This is an insightful suggestion. We have now explicitly included this topic within our discussion section.

Reviewer #3:

Manuscript Summary:

In this manuscript titled "A live-cell imaging approach for real-time high throughput fluorescent measurement of synaptic functions in models of ALS/FTD", Krishnamurthy et al. described two fluorescent based methods to quantify neuronal activity and synaptic physiology induced by high KCl in cultured neurons. First, they demonstrated synaptic vesicle release using FM4-64 dye, which labels synaptic vesicle membranes. Second, they measured calcium influx using Gcamp6m, a fluorescent Ca^{2+} reporter. They proposed that these methods could be used for high throughput screen in multiple cellular models like rodent primary neurons and human iPSC-derived neurons and serve as a first indicator of synaptic abnormality in neurodegeneration, due to its relatively low cost and easy technical accessibility. It true, this platform can be useful for various diseases beyond ALS/FTD and is readily adaptable for different cellular models. The manuscript is well written with several published papers as a backup. Although using membrane dye and Gcamp probes to assess synaptic function is not new and has been routinely used in many labs in a high content format, it is nice to have detailed protocols describing these methods in a systematic way. Therefore, this manuscript is of interest to the field and may provide useful resources for the neurodegeneration research community.

Major Concerns:

1. The authors suggested that these methods are highly reproducible, however, this should be demonstrated better with statistical analysis over multiple biological repeats and technical repeats. 30 neurons over 3 experiments were not enough and it was not clear how reproducibility was confirmed, as both biological and technical repeats should be included and compared.

We value this input and have now been more explicit as to how technical and biological replicates are performed for the published studies we have reported^{1,2}. The situations we have probed have quite dramatic changes and so n=3 biological replicates each with technical replicates of 10 neurons and 5 ROIs per neuron per condition have been sufficient for reproducible, statistically significant effects. We have added a note for experimenters as well, that if more subtle phenotypes are investigated, the number of biological and/or technical replicates may need to be altered.

2. The authors focused on C9-GA peptides, however, GP and PA also produce toxicity in a faster and more robust way. It would be nice to compare the effects of all 3 peptides and evaluate the robustness and sensitivity of the two assays.

We appreciate this feedback and have thought extensively on this topic in the past. The focus on poly-GA within this manuscript is for the purpose of illustrating effectiveness of the method in the context of a "positive" control GFP cell, and a "dysfunctional" poly-GA containing cell. Thus, comparing the toxicity of GA vs other DPRs is beyond the scope of this manuscript. Of note, in the published work from which this data is drawn, we have discussed thoroughly why GA was explored compared to the other dipeptide repeats¹. Briefly, we observe punctate poly-GA in neurites, suggesting there may be synaptic interactions. Additionally, the robust and rapid toxicity of the arginine containing repeats (GR, PR) preclude them from being examined in this manner, as we wished to explore synaptic deficits prior to any overt neuronal toxicity. In our hands, we have not witnessed toxicity from PA or GP in cortical or motor neurons and observed them in a diffuse staining pattern and so did not pursue them in our continued evaluation of synaptic effects³. Nevertheless, we do value the comment regarding demonstrating the sensitivity of our assays. We have now also included our rescue experiment studies from our published work as representative data in Figure 3, to show that we are able rescue the synaptic dysfunction phenotype and have intermediate effects compared with the "all or nothing" response previously shown in present Figure 3F¹. From this published work, we have also now included conditions with and without bath calcium to demonstrate sensitivity of our calcium imaging paradigm in Figure 4D¹.

3. Some critical details about imaging are missing, e.g. how was background extraction performed (was background value different for each frame and extracted separately)? How was fluorescence intensity measured and compared (max vs. mean vs. median vs. sum)? The authors stated that they were using a frame rate of 500msec, did that mean 1 frame every 500msec (it would be better to describe frame rate as fps in this case)? What about the exposure time? Were any z-stacks taken and MPI used? The authors stated that "confocal aperture is set to 1 (an arbitrary unit) to achieve optimal resolution of neurites, however, the object here is not the neurite but the fluorescent puncta (positive for the FM dye or Gcamp6m), this needs to be clarified. Also what resolution? Spatial or temporal?

In critically reading our protocol, we have addressed the above concerns. An explicit description of background subtraction is included in step 8.6. We report the fluorescence intensity as "raw fluorescence intensity" as is measured by our software for each frame captured. We have adjusted our description of frame rate to be 2 frames per second by the camera and clarified a 200 msec exposure time. For all experiments, we only imaged from a single plane because z-stack imaging prohibits temporal resolution of synaptic transmission. A description is now included that a single plane was used, with no z-stacks captured due to speed of imaging. This is highlighted in the importance of using perfect focus in step 5.5. We have clarified what we mean by our confocal aperture setting, and that we do so to enable proper visualization of fluorescent puncta within neurites. We set the confocal aperture to 1 based on the software recommendation for our objective (40 X oil immersion objective with a numerical aperture of 1) to achieve the best possible spatial resolution and to avoid overlap of fluorescent puncta. However, this confocal aperture can be adjusted according to the objective used. We have specified that either 20x or 40x objectives may be used, with temporal imaging settings.

4. The specificity and sensitivity of the FM4-64 dye needs to be thoroughly reviewed and critically discussed as they may also label other lipid membranes. In addition, its decrease in intensity should be carefully examined to determine whether it was due to vesicle release or photo bleaching, some counterstaining of synaptic vesicles and a better described correlation between the kinetics of dye intensity and synaptic recycle may help.

We thank the reviewer for these suggestions and value this concern for the specificity of FM4-64 dye. We acknowledge that this type of dye can label other lipid membranes, however others have already detailed the utility of such dyes for labeling synaptic vesicles and usage in similar assays⁴⁻⁷. These dyes have already been extensively used to study neuronal synaptic vesicle dynamics in primary neurons and at the neuromuscular junction⁸⁻¹⁶. We have made sure to include such references in the introduction of these dyes. We have also included reference of published work explicitly co-staining such dye with synaptic vesicle marker proteins⁹, and in-house staining that we have recently performed. Figure 2 now shows an experiment done to validate the specificity of FM4-64 styryl dye labeling in primary rodent cortical neurons. As explained in detail in our protocol, we transfected cortical neurons with a fluorescently tagged (mTurquoise2) plasmid construct encoding the presynaptic terminal marker protein synaptophysin and, 24 hours later, loaded the neurons with FM4-64. A majority of FM4-64 puncta co-localize with synaptophysin puncta (Figure 2A), confirming the specificity of labelling that has been extensively described as reported above.

We have also made a specific note regarding laser power and "non-stimulation" controls to avoid the potential for photobleaching following step 5.3. An additional note is included following step 6.6, to ensure that passive dye diffusion and photobleaching are not occurring prior to stimulation. As a further measure to show that photobleaching is not occurring, we also show an additional control experiment to rule out the possibility that FM4-64 unloading upon KCl depolarization could be related to photobleaching (Figure 2B-C). As described in the protocol, we performed simultaneous fluorescence imaging of FM4-64 styryl dye and synaptophysin- mTurquoise2. mTurquoise fluorescence is very dim, and laser power for this channel was significantly higher than that of the TRITC FM4-64. Loss of FM4-64 fluorescence intensity after KCl depolarization is strikingly high compared to that of synaptophysin-

mTurquoise2. Therefore, taking this experiment as well as our other controls of stable fluorescence prior to stimulation and “non-stimulation” wells, we have established through our settings that decreases in FM4-64 fluorescence can be attributed to synaptic unloading through KCl depolarization rather than photobleaching effects.

5. Potential bias and how to reduce bias should be better discussed, as this is critical for any imaging methods.

We thank the reviewer for bringing up this point. We have included details of experimental blinding following steps 6.8 and 7.6 to reduce potential bias.

Minor Concerns:

1. In the primary culture protocol, the authors used papain for digestion but then used trypsin inhibitor later. Which enzyme was used? Trypsin or Papain?

We appreciate the reviewer pointing this out. We updated our protocol to include papain instead of trypsin, and did not remove the mention of trypsin inhibitor from our master protocol. This has now been fixed in-text.

2. As the authors pointed out, transfection may be potentially problematic in neurons, it will be informative to describe the transfection efficiency using different methods and evaluate the heterogeneity due to the different levels of probe expression.

We appreciate this suggestion. As was stated for Reviewer #1, mention of these details is now included in the discussion section regarding transfection efficiency. Neuronal transfection is very challenging, and within our laboratory only Lipofectamine based method attains efficiencies between 15% to 25%. As our GCaMP transfection typically reaches 20-25% of cells, we have not tested other transfection protocols. If higher numbers of reporter neurons are necessary, we would suggest using the viral vector transduction method described within our discussion.

3. It is unclear why the authors used CO₂ to solubilize Ca(OH)₂ instead of using a fresh bottle, because this method will yield Ca(HCO₃)₂ instead of CaCl₂ and this addition may affect neurons and medium pH.

We value this comment and have incorporated this point as a note for that protocol step. As you have recommended we have suggested always using a fresh bottle. We have now included the rationale for the carbonation step, and stressed the necessity of checking pH following this step as excessive carbonation can surpass solubilizing surface Ca(OH)₂ and produce Ca(HCO₃)₂ as mentioned.

Reviewer #4:

Manuscript Summary:

Krishnamurthy et al. describe a protocol for the live-cell imaging of synaptic vesicle release and calcium dynamics in primary cortical and motor neurons. This protocol will be a very useful and significant resource for the field. However, the impact of this protocol could be extended with an explicit description of the models of ALS/FTD used by the authors. There are also several minor concerns that need to be addressed.

Major Concerns:

1. The title, abstract, and introduction emphasize the use of this live-cell imaging protocol in models of ALS/FTD. However, specifics are not provided on which plasmids are used to express disease-associated proteins to examine models of ALS/FTD. Providing this information would substantially increase the impact of this protocol for investigators interested in studying models of ALS/FTD. Some constructs are briefly mentioned in the figure legends, but the methods list only vague terminology for an “mcherry tagged ALS/FTD plasmid of interest” (line 307). This information should be expanded to describe in

detail possible models of disease and what specific mutants of each disease could be used. Furthermore, are GFP-tagged plasmids used in combination with FM4-64 labeling? Please clarify.

We appreciate this feedback and have now included details of all plasmids used to demonstrate representative results and ALS-relevance to the protocols described. Within our discussion we have extended potential applications to describe a larger scope of ALS genetic mutations (and other neurological disorders) which could be studied using these methods. We have also been clearer in indicating that we have used GFP plasmids with FM4-64 (styryl dye) imaging and mCherry plasmids with GCaMP imaging, and have indicated as a note to future experimenters to keep in mind the limitation of ensuring there is no conflict with the fluorophore of the imaging indicator.

2. The abstract and introduction are written as if live cell imaging is a new technology, but has been around for over a decade at least. Perhaps the authors can remove these references and jump directly into the strengths of live cell imaging and probes to be covered. Example: line 30-32, "With new microscope technology, coupling confocal imaging with precise monitoring and manipulation of physiological parameters like temperature and CO₂, real-time investigation of the inner workings of live cells is now possible."

We agree that we do not wish to portray live-imaging technology as a recent technology. We have removed the suggested lines from our abstract and introduction to focus more on the specific protocols and probes we describe within the article. These sections now read that the styryl dye and GCaMP reporter we now use are the latest iterations and are more specific than previous versions.

Minor Concerns:

1. Concentrations of poly-lysine and laminin should be stated.

These concentrations are now included.

2. Figures are low resolution, making it difficult to assess the information. Higher resolution images should be provided.

We apologize for this oversight. The rapid imaging rate used on 20x images results in the imaging resolution shown in our original submission. We have now included 40x images in Figures 3D and 4A to illustrate the same concepts.

3. Image analysis (step 8):

a. Can the authors provide more information on how the ROI location is chosen for the FM4-64 images?

We have addressed this point by including a note following step 8.3, where we described neuronal tracks outlined by a brightfield still image and regions selected by choosing regions with distinct separated puncta.

b. In the calculations for $\Delta F/F$, is the "baseline fluorescence value" that is generated by averaging the last 30 seconds (used in steps 7 and 8), normalized to background like the data in step 6? Please clarify.

We have now included more details for this entire section as to how data was analyzed step-by-step. We have clarified that the raw background ROI has first been subtracted out from the entirety of the recording period. We also have also noted explicitly that the "baseline fluorescence value" generated from the final 30 seconds is also subtracted from the entirety of the basal and stimulated periods.

c. Please justify the use of 30 second intervals to generate the mean baseline fluorescence value. In the case of GCaMP6 - are there no firing events during this time to affect the mean value?

We have addressed both of these points as notes within the protocol section. Establishment of a basal baseline period without firing events/associated calcium transients is following step 7.5. Usage of data from the final 30 seconds of basal recording is justified following step 8.7.

4. Throughout the manuscript, the term "data" is not treated as plural.

We have proofread these occurrences and fixed them.

5. Identify the scale bar in Figure 3A in the legend.

As mentioned in point 2 we have switched out this image to be higher resolution. This new image contains the associated scale bar, which is indicated in the figure legend.

6. In Figure 2F and Figure 3C, the y-axis title should specify the marker quantified.

These two figures were drawn from previously published Figures and were inserted as shown in those publications. However, we appreciate this critique and have now included the type of imaging performed on the y-axis for this article.

7. Table 2 title should read "Composition of artificial cerebrospinal fluid (aCSF) buffers".

We have adjusted this title accordingly.

8. For clarity, the justification for the aCSF needing to be made fresh prior to each round of experiments should be reiterated in the discussion (lines 481-483).

The description of the importance of preparing fresh aCSF prior to each round of experiments is included in the discussion section.

9. Perhaps it would be more clear to write frame rate as "2 frames per second", instead of 500 msec which can be confused with exposure time?

As was mentioned for Reviewer #3, we agree with this shift in describing frame rate and have amended the protocol accordingly.

10. Data analysis should be step No. 9 and not 8.

Thank you for catching this oversight, it has now been fixed.

- 1 Jensen, B. K. *et al.* Synaptic dysfunction induced by glycine-alanine dipeptides in C9orf72-ALS/FTD is rescued by SV2 replenishment. *EMBO Molecular Medicine*. **12** (5), e10722, (2020).
- 2 Kia, A., McAvoy, K., Krishnamurthy, K., Trotti, D. & Pasinelli, P. Astrocytes expressing ALS-linked mutant FUS induce motor neuron death through release of tumor necrosis factor-alpha. *Glia*. **66** (5), 1016-1033, (2018).
- 3 Wen, X. *et al.* Antisense proline-arginine RAN dipeptides linked to C9ORF72-ALS/FTD form toxic nuclear aggregates that initiate in vitro and in vivo neuronal death. *Neuron*. **84** (6), 1213-1225, (2014).
- 4 Gaffield, M. A. & Betz, W. J. Imaging synaptic vesicle exocytosis and endocytosis with FM dyes. *Nature Protocols*. **1** (6), 2916-2921, (2006).
- 5 Verstreken, P., Ohyama, T. & Bellen, H. J. FM 1-43 labeling of synaptic vesicle pools at the Drosophila neuromuscular junction. *Methods Molecular Biology*. **440** 349-369, (2008).
- 6 Angleson, J. K. & Betz, W. J. Monitoring secretion in real time: capacitance, amperometry and fluorescence compared. *Trends in Neuroscience*. **20** (7), 281-287, (1997).
- 7 Betz, W. J. & Bewick, G. S. Optical monitoring of transmitter release and synaptic vesicle recycling at the frog neuromuscular junction. *Journal of Physiology*. **460** 287-309, (1993).
- 8 Ryan, T. A. *et al.* The kinetics of synaptic vesicle recycling measured at single presynaptic boutons. *Neuron*. **11** (4), 713-724, (1993).
- 9 Kraszewski, K. *et al.* Synaptic vesicle dynamics in living cultured hippocampal neurons visualized with CY3-conjugated antibodies directed against the luminal domain of synaptotagmin. *Journal of Neuroscience*. **15** (6), 4328-4342, (1995).
- 10 Betz, W. J., Mao, F. & Bewick, G. S. Activity-dependent fluorescent staining and destaining of living vertebrate motor nerve terminals. *Journal of Neuroscience*. **12** (2), 363-375, (1992).
- 11 Betz, W. J. & Bewick, G. S. Optical analysis of synaptic vesicle recycling at the frog neuromuscular junction. *Science*. **255** (5041), 200-203, (1992).
- 12 Ryan, T. A. & Smith, S. J. Vesicle pool mobilization during action potential firing at hippocampal synapses. *Neuron*. **14** (5), 983-989, (1995).
- 13 Betz, W. J., Ridge, R. M. & Bewick, G. S. Comparison of FM1-43 staining patterns and electrophysiological measures of transmitter release at the frog neuromuscular junction. *Journal of Physiology-Paris*. **87** (3), 193-202, (1993).
- 14 Wu, L. G. & Betz, W. J. Nerve activity but not intracellular calcium determines the time course of endocytosis at the frog neuromuscular junction. *Neuron*. **17** (4), 769-779, (1996).
- 15 Ryan, T. A., Smith, S. J. & Reuter, H. The timing of synaptic vesicle endocytosis. *Proceedings of the National Academy of Sciences of the United States of America*. **93** (11), 5567-5571, (1996).
- 16 Ramaswami, M., Krishnan, K. S. & Kelly, R. B. Intermediates in synaptic vesicle recycling revealed by optical imaging of Drosophila neuromuscular junctions. *Neuron*. **13** (2), 363-375, (1994).



Synaptic dysfunction induced by glycine-alanine dipeptides in C9orf72-ALS/FTD is rescued by SV2 replenishment

Author: Brigid K Jensen, Martin H Schuld, Kevin McAvoy, et al

Publication: EMBO Molecular Medicine

Publisher: John Wiley and Sons

Date: Apr 29, 2020

© 2020 The Authors. Published under the terms of the CC BY 4.0 license

Open Access Article

This is an open access article distributed under the terms of the [Creative Commons CC BY](#) license, which permits unrestricted use, distribution, and reproduction in any medium, provided the original work is properly cited.

You are not required to obtain permission to reuse this article.

For an understanding of what is meant by the terms of the Creative Commons License, please refer to [Wiley's Open Access Terms and Conditions](#).

Permission is not required for this type of reuse.

Wiley offers a professional reprint service for high quality reproduction of articles from over 1400 scientific and medical journals. Wiley's reprint service offers:

- Peer reviewed research or reviews
- Tailored collections of articles
- A professional high quality finish
- Glossy journal style color covers
- Company or brand customisation
- Language translations
- Prompt turnaround times and delivery directly to your office, warehouse or congress.

Please contact our Reprints department for a quotation. Email corporatesaleseurope@wiley.com or corporatesalesusa@wiley.com or corporatesalesDE@wiley.com.



Astrocytes expressing ALS-linked mutant FUS induce motor neuron death through release of tumor necrosis factor-alpha

Author: Piera Pasinelli, Davide Trotti, Karthik Krishnamurthy, et al

Publication: GLIA

Publisher: John Wiley and Sons

Date: Jan 30, 2018

© 2018 The Authors. Glia Published by Wiley Periodicals, Inc.

Quick Price Estimate

Content Delivery:

A copy of this content may be purchased following completion of your permissions order.
High Res Image files - please contact Wiley

Please review the credit line for the requested figure/table.
If the figure/table you wish to reproduce is credited to a source other than the author of the publication (i.e third party material) you will need to obtain permission from that copyright holder, book or journal before making any use of the material. For the avoidance of doubt - any and all third party content is expressly excluded from this permission.
Otherwise please proceed with your order.

As the Author of this content you retain the right to re-use the final version (or parts thereof) in any new publication you are authoring, co-authoring or editing (excluding journal articles) where the re-used material constitutes less than half of the total material in the publication. In such case, any modifications should be accurately noted.
If you still require a license, please proceed with your order. You will not be charged for this permission.

I would like to...

reuse in a journal/magazine

Number of figures/tables

1

Requestor Type

Author of this Wiley article

Will you be translating?

No

Is the reuse sponsored by or associated with a pharmaceutical or medical products company?

No

Circulation

200 - 499

Select your currency

USD - \$

Format

Electronic

Quick Price

0.00 USD

Portion

Figure/table

QUICK PRICE

CONTINUE

Information regarding permissions for developing countries.